# $O_2$ Activation and Aromatic Hydroxylation Performed by Diiron Complexes

**Stéphane Ménage,[†] Jean-Baptiste Galey,[‡] Jacqueline Dumats,[‡] Georges Hussler,[‡] Michel Seité,[‡] Isabelle Gautier Luneau,[§] Geneviève Chottard,[⊥] and Marc Fontecave*[,†]**

*Contribution from the Laboratoire de Chimie et Biochimie des Centres Redox Biologiques, DBMS-CEA Grenoble/EP 1087 CNRS/ Université Joseph Fourier, 17 Rue des Martyrs 38054, Grenoble Cédex 9, France, L'Oréal Research Center, 1 avenue Eugène Schueller, 93600 Aulnay sous bois, France, L.E.D.S.S., UMR 5616, Université Joseph Fourier, 301 rue de la Chimie, 91041 Grenoble Cedex, France, and Laboratoire de Chimie des Métaux de Transition, Université Pierre et Marie Curie, F75230 Paris Cedex 05, France*

*Received April 3, 1998*

**Abstract:** Chemical models of active sites of diiron oxo proteins have been synthesized. The polydendate ligands are EDTA derivatives which provide a balanced supply of nitrogen atoms and carboxylate groups together with an oxidizable phenyl moiety, thus mimicking both the iron coordination in methane monooxygenase and a nearby substrate site. All the diferric complexes have been characterized in solution by ESI-MS, optical absorption, and in some cases by $^1$H NMR. In the case of the ligand **L1** [**L1** = (*N*,*N*′-bis(3,4,5-trimethoxybenzyl)-ethylenediamine *N*,*N*′-diacetic acid)], the X-ray structure of the corresponding iron complex has been determined, revealing an original tetranuclear unit, $Fe_4O_2(\mathbf{L1})_4 \cdot 10H_2O$, issued from the dimerization of two $[Fe_2O(\mathbf{L1})_2]$ units linked by carboxylate bridges. In a solution containing water or acetate, the tetranuclear complex decomposed into dinuclear complexes, which proved to be able to react with hydrogen peroxide or dioxygen in the presence of ascorbate. The final product was a mononuclear complex identified as $[Fe(III)\mathbf{L'1}(H_2O)]$ with **L′1** resulting from the quantitative hydroxylation of **L1**. The complex and the oxidized ligand were characterized by EPR, NMR, and UV−vis spectroscopies and by mass spectrometry. Labeling experiments showed that with both $H_2O_2$ or $O_2$ and ascorbate, the incorporated oxygen came from the oxidant exclusively. This reaction mimicks the transformation of a tyrosine residue, brought into proximity of the active center of Ribonucleotide reductase of *Escherichia coli* by site-directed mutagenesis, into 3,4-dihydroxyphenylalanine.

## Introduction

Oxygen-activating enzymes with dinuclear non heme iron active sites, in which two iron(III) atoms are bridged by an oxo or an hydroxo group in their resting state, participate in many metabolic important reactions.[1] Despite similar active centers, these so-called diiron oxo enzymes present a considerable range of activities, from redox chemistry to hydrolysis of phosphodiesters (purple acid phosphatase)[2] and dioxygen transport (hemerythrin).[3] Ribonucleotide reductase (RNR) (class I) catalyzes the reduction of ribonucleotides into deoxyribonucleotides, the DNA precursors.[4] Enzyme activation consists of a one-electron oxidation of an endogenous tyrosine residue effected in the small subunit by a dinuclear iron site and molecular oxygen to initiate a radical chemistry on the large subunit.[5] Methane monooxygenase (MMO), isolated from methanotrophic organisms catalyzes the transformation of methane into methanol using molecular oxygen as the oxidant in the presence of a source of electrons.[6] A great variety of alkanes are also substrates for MMO.[7] Furthermore, hydrogen peroxide as well can be used as the oxidant, with no need for a reducing agent. A growing number of enzymes belonging to this class of proteins catalyzes various reactions: toluene 2- or 4-monooxygenase (aromatic hydroxylation of toluene);[8] alkene monoxygenase;[9] membrane stearoyl-CoA $\Delta^9$ desaturase (incorporation of double bonds).[10] Nature seems then to have selected an alternative active center to perform activities previously described for cytochrome P450 and related heme enzymes.[11]

[†] EP 1087 CNRS, Université Joseph Fourier, CEA Grenoble.
[‡] L'Oréal Research Center.
[§] L.E.D.S.S., Université Joseph Fourier.
[⊥] Université Pierre et Marie Curie.

(1) (a) Kurtz, D. M., Jr. *J. Biol. Inorg. Chem.* **1997**, *2*, 159. (b) Feig, A. L.; Lippard, S. J. *Chem. Rev.* **1994**, *94*, 759. (c) Que, L., Jr.; True, A. E. *Prog. Inorg. Chem.* **1990**, *38*, 97. (d) Wallar, B. J.; Lipscomb, J. D. *Chem. Rev.* **1996**, *96*, 2625.

(2) (a) Doi, K.; Antanaitis, B. C.; Aisen, P. *Struct. Bonding* **1988**, *70*, 1. (b) Vincent, J. B.; Ollivier-Lilley, G. L.; Averill, B. A. *Chem. Rev.* **1990**, *90*, 1447. (c) Sträter, N.; Klabunde, T.; Tucker, P.; Witzel, H.; Krebs, B. *Science* **1995**, *268*, 1489.

(3) Stenkamp, R. E. *Chem. Rev.* **1994**, *94*, 715.

(4) (a) Fontecave, M.; Nordlund, P.; Eklund, H.; Reichard, P. *Adv. Enzymol*. **1992**, *65*, 147. (b) Sjoberg, B.-M. *Structure Bonding* **1997**, *88*, 139.

(5) (a) Sturgeon, B. E.; Burdi, D.; Chen, S.; Huynh, B.-H.; Edmondson, D. E.; Stubbe, J.; Hoffman, B. M. *J. Am. Chem. Soc*. **1996**, *118*, 7551. (b) Tong, W. H.; Chen, S.; Lloyd, S. G.; Edmondson, D. E.; Huynh B. H.; Stubbe, J. *J. Am. Chem. Soc.* **1996**, *118*, 2107.

(6) (a)Woodland, M. P.; Dalton, H. *J. Biol. Chem*. **1984**, *259*, 53. (b) Rosenzweig, A. C.; Frederick, C. A.; Lippard, S. J.; Nordlund, P. *Nature* **1993**, *363*, 537.

(7) Green, J.; Dalton, H. *J. Biol. Chem*. **1989**, *264*, 17698.

(8) (a) Newman, L. M.; Wackett, L. P. *Biochemistry* **1995**, *34*, 14066. (b) Pikus, J. D.; Studts, J. M.; Achim, C.; Kauffmann, K. E.; Münck, E.; Steffan, R. J.; McClay, K.; Fox, B. G. *Biochemistry* **1996**, *35*, 9106.

(9) Shanklin, J.; Whittle, E.; Fox, B. G. *Biochemistry* **1994**, *33*, 12787.

(10) Fox, B. G.; Shanklin, J.; Somerville, C.; Münck, E. *Proc. Natl. Acad. Sci. U.S.A.* **1993**, *90*, 2486.

(11) (a) Sono, M.; Roach, M. P.; Coulter, E. D. Dawson, J. H. *Chem. Rev.* **1996**, *96*, 2841. (b) Meunier, B. *Chem. Rev.* **1992**, *92*, 1411 and references therein.

10.1021/ja981123a CCC: $15.00 
Published on Web 12/30/1998

The enzymatic mechanism of MMO and related enzymes has been partially elucidated by stopped flow kinetic studies. Some key intermediates have been identified but the mechanism of the hydrocarbon C−H bond cleavage and the C−O bond formation remains unknown. Dioxygen binds to the diferrous active site leading to the first intermediate, compound P, characterized as a $\mu$-peroxo diferric center.[1d,12] Compound P decays to compound Q, identified as a coupled $Fe(IV)_2$ unit.[13] It has been proposed that the reaction products are derived from the 2-electron oxidation of the substrate by compound Q. The reaction of Q with the substrate has not been clarified yet. Up to now, both H• abstraction (radical chemistry) or concerted mechanisms (non-radical chemistry) have been proposed.[1d]

Chemical models of diiron oxo proteins proved to have the potential to catalyze alkane oxidation by hydrogen peroxide, alkylhydroperoxides, and peracids.[14] However, still very few homogeneous systems are able to activate molecular oxygen in the presence of a reducing agent and to oxidize substrates, as does the enzyme.[15] The reactions are extremely slow, and yields are exceedingly small. The critical step is probably not the oxygen activation itself but rather the transfer of oxygen atom to the substrate. As a matter of fact, the homogeneous reaction mixture contains large excesses of the reducing agent which is much less resistant to oxidation, by definition, and thus competes with the substrate efficiently. To solve this problem, oxygenases have closely combined the metal site and the substrate binding site, resulting in a very high local substrate concentration, and set up mechanisms for finely tuning the electron flow.

To approach this situation, we have selected polydentate ligands containing both carboxylate and nitrogen chelating moieties, which better mimic the glutamate/aspartate/histidine coordination environment in MMO and RNR. Furthermore, these ligands also contain an oxidizable phenyl group, mimicking the protein-bound substrate. Phenyl groups have been chosen as to model benzene hydroxylation by MMO[6] and the transformation of a tyrosine residue, brought into proximity of the active center of RNR by site directed mutagenesis, into 3,4-dihydroxyphenylalanine (dopa).[16]

This approach has been successful so far with the ligand **L1** (*N*,*N*′-bis(3,4,5-trimethoxybenzyl)ethylenediamine *N*,*N*′-diacetic acid), an EDTA derivative in which two carboxylato arms have been replaced by two phenyl groups. In the presence of acetate, an iron salt, and **L1**, a $\mu$-oxo-$\mu$-acetato diferric complex, **2**, has been characterized. In a water:acetonitrile mixture, this complex reacts with hydrogen peroxide to oxidize one of the phenyl moieties into a phenol. As a result, the complex breaks down into a mononuclear species in which the phenolate is bound to the ferric ion. More interesting, the same transformation was observed with ascorbate in the presence of air.[17]

In this paper, we present our investigation on the first example of a quantitative ligand hydroxylation within a diiron complex by $O_2$ in aqueous solutions, which can be regarded as an original model of monooxygenases. Only very few studies on diiron complexes as oxidation catalysts in aqueous solution have been reported so far.[18] We concentrated on the isolation and full characterization of the iron complex **2** and its oxidation product. By synthesizing a variety of **L1** analogues, a structure/reactivity study could be performed in order to have an insight into the structural parameters which influence the stability and the reactivity of the diiron complex. From these results, a mechanism is proposed.

## Experimental Section

**Physical Methods.** Starting materials were purchased from Fluka or Sigma Aldrich Co. Column chromatography utilized Merck silica gel (230−400 mesh). Melting points are uncorrected. $^1$H and $^{13}$C NMR spectra were recorded on Brucker 500, 400, or 200 MHz spectrometers. Chemical shifts (ppm) for paramagnetic species were referred to residual protic solvent peaks. EPR spectra were recorded with a Varian E102 at $T = 4$ K or a Bruker ESP 300E at $T = 100$ K and ambient temperature (spin trapping experiments). All elemental analysis are within 0.4% of the calculated values unless otherwise specified. UV−visible spectra were recorded with a Perkin-Elmer Lambda 2S or a Uvikon 930 spectrophotometer. Mass spectra were obtained either by desorption chemical ionization (DCI) or electron impact ionization (EI) with a Finnigan Mat SSQ 710 mass spectrometer or by HPLC/MS with a Fisons Platform mass spectrometer equipped with an atmospheric pressure ion source in the electrospray ionization (ESI) mode.

Optimized ionization conditions for ESI-MS have been obtained for 0.1 mM of compounds using a syringe pump with a 3 $\mu$L min$^{-1}$ flow rate. The analysis have been performed in profile (MCA mode, 3 s per 500 uma and the spectra of positive and negative mode correspond to the sum of 15−20 recorded spectra. Calibrations have been done with a 2000 ppm solution of NaI and 10 ppm solution of CsI in a water/2-propanol 50:50 mixture for a mass range between 500 and 1500. From the range of 1500−3000, bovin trypsinogen has been used for calibration. Capillary tension: 3.8 kV. Source temperature: 50 °C. Cone voltage: 20 to 70 V. The fragmentation studies of complex **3** have been performed by FAB/MS/MS using a TSQ700 (Finnigan MAT) mass spectrometer (collision gas:argon). Conversion of complex **1** or **2** into **3** in a water:acetonitrile mixture has been followed at −10 °C using the technique developed by Kim et al.[19] The mixing of the oxidant and the starting complex was effected in the mixing chamber using a mixing tee.

The RR spectra were obtained on a J. Y. U1000 double monochromator, equipped with an AsGa photomultiplier and photon-counting electronics. The violet lines (413.1 and 406.7 nm) from a $Kr^+$ laser were used as excitation lines at 10−15 mW power. The spectral slit width was 6 cm$^{-1}$ at 406.7 nm. The complex was studied in solution (2 mM in 50 mM acetate buffer), in a rotating cell. The solution was renewed after 5 min exposure to the laser light to prevent photodecomposition of the sample.

**Ligand Synthesis.** Ligands **L1**, **L2**, **L3**, and **L5** were prepared by reacting bromoacetic acid with the corresponding diamines obtained by reductive alkylation of the appropriate aldehydes. Compound **L6** was obtained by reacting 2-picolyl chloride with the corresponding diamine. Synthesis of compound **L7** was performed starting from monoacetylated ethylenediamine. Attempts to obtain **L7** free of salts from alkylation with bromoacetic acid were unsuccessful. Therefore *tert*-butyl chloroacetate was used, followed by acid hydrolysis. All

(12) (a) Lee, S.-K.; Neisheim, J. C.; Lipscomb, J. D. *J. Biol. Chem.* **1993**, *268*, 21569. (b) Liu, S. J.; Valentine, A. M.; Qiu, D.; Edmondson, D. E.; Appelman, E. H.; Spiro, T. G.; Lippard, S. J. *J. Am. Chem. Soc.* **1995**, *11*, 4997.

(13) (a) Liu, K. E.; Valentine, A. M.; Wang, D.; Huynh, B. H.; Edmondson, D. E.; Salifoglou, A.; Lippard, S. J. *J. Am. Chem. Soc.* **1995**, *117*, 10174. (b) Lee, S.-K.; Fox, B. G.; Froland, W. A.; Lipscomb, J. D.; Münck, E. *J. Am. Chem. Soc.* **1993**, *115*, 6450. (c) Shu, L.; Nesheim, J. C.; Kauffman, K.; Münck, E.; Lipscomb, J. D.; Que, L., Jr. *Science* **1997**, *275*, 515.

(14) (a) Buchanan, R. M.; Chen, S.; Richardson, J. F.; Bressan, M.; Forti, L.; Morvillo, A.; Fish, R. H. *Inorg. Chem.* **1994**, *33*, 3208. (b) Kim, J.; Harrison, R. G.; Kim, C.; Que, L., Jr. *J. Am. Chem. Soc.* **1996**, *118*, 4373. (c) Duboc-Toia, C.; Ménage, S.; Lambeaux, C.; Fontecave, M. *Tetrahedron Lett.* **1997**, *38*, 3727 and references therein. (d) Kodera, M.; Shimakoshi, H.; Kano, K. *J. Chem. Soc., Chem. Commun.* **1996**, 1737.

(15) (a) Vincent, J. B.; Huffman, J. C.; Christou, G.; Li, Q.; Nanny, M. A.; Hendrickson, D. N.; Fong, R. H.; Fish, R. H. *J. Am. Chem. Soc.* **1988**, *110*, 6898. (b) Tabushi, I.; Nakajima, T.; Seto, K. *Tetrahedron Lett.* **1980**, *21*, 2565. (c) Kitajima, N.; Ito, M.; Fukui, H.; Moro-oka, Y. *J. Chem. Soc., Chem. Commun.* **1991**, 102.

(16) Åberg, A.; Ormö, M.; Nordlund, P.; Sjöberg, B.-M. *Biochemistry* **1993**, *32*, 9845.

(17) Ménage, S.; Galey, J.-B.; Hussler, G.; Seité, M.; Fontecave, M. *Angew. Chem., Int. Ed. Engl.* **1996**, *35*, 2353.

(18) Rabion, A.; Chen, S.; Wang, J.; Buchanan, R. M.; Seris, J.-L.; Fish, R. H. *J. Am. Chem. Soc.* **1995**, *117*, 12356.

(19) Kim, J.; Larka, E.; Que, L., Jr. *Inorg. Chem.* **1996**, *35*, 2369.

attempts to prepare **L4** by the same method using 3-bromopropionic acid were unsuccessful, and finally it was synthesized by alkylation of diethyl ethylenediamine *N,N′*-dipropionate using 3,4,5-trimethoxybenzyl chloride followed by hydrolysis of the ester.

**General Procedure for Preparing 3,4,5-Substituted *N,N′*-Dibenzylidenealkylenediamine *N,N′*-diacetic L1, L2, L3, and L5. (a)** To a stirred solution of 250 mmol of the required benzaldehyde in 300 mL of methanol, 125 mmol (0.5 equiv) of alkylenediamine were added dropwise. The reaction mixture was stirred for 1 h at room temperature and then cooled at 5 °C. The Schiff base was collected by filtration and washed extensively with cold methanol to yield a crystalline powder. In some cases the diimine did not crystallize, and the product was obtained as a crude oil after evaporation of the solvent.

**(b)** To a stirred suspension of 40 mmol of diimine in 300 mL of ethanol 2.27 g (60.0 mmol) of $NaBH_4$ was added portionwise. The reaction mixture was stirred at 55−60 °C for 2 h and then allowed to stand at room temperature for 1 h. HCl (6 N) was then slowly added to adjust the pH of the solution to 1. The crystalline diamine dihydrochloride was collected by filtration, washed with cold ethanol, and vacuum dried over $P_2O_5$.

**(c)** Diamine dihydrochloride (28.4 mmol) was dissolved in 140 mL of water containing 7.50 mL of 30% sodium hydroxide. To a stirred solution of 7.88 g of bromoacetic acid (56.8 mmol) in 16 mL water was added 4.76 g of $NaHCO_3$ portionwise at 0 °C. The two solutions were mixed, and the resulting mixture was heated to 40 °C for 4 h. Aqueous NaOH (30% solution) was used to maintain the pH of the solution in the range of 10−11 throughout. The mixture was cooled and acidified with concentrated HCl (pH 2). The white precipitate was filtered and dried. Final products were usually obtained as mixtures of hydrochlorides and free bases. Some compounds contained small amounts of hydrobromide.

***N,N′*-Bis(3,4,5-trimethoxybenzyl)ethylenediamine *N,N′*-Diacetic Acid Dihydrochloride (L1). (a)** *N,N′*-Bis(3,4,5-trimethoxybenzylidene)ethylenediamine was prepared according to the general procedure from 3,4,5-trimethoxybenzaldehyde (50.0 g, 255 mmol) and ethylenediamine as a pale yellow powder (49.4 g, 93%): mp 148 °C; $^1$H NMR (500 MHz, DMSO-$d_6$) $\delta$ 3.70 (s, 6H), 3.80 (s, 12H), 3.85 (s, 4H), 7.04 (s, 4H), 8.26 (s, 2H); MS (EI) *m/z*: 416, [$M^{+\bullet}$].

**(b)** *N,N′*-Bis(3,4,5-trimethoxybenzyl)ethylenediamine dihydrochloride was obtained from the corresponding diimine (20.0 g, 48.0 mmol) according to the general procedure as a white solid (19.5 g, 96%): $^1$H NMR (500 MHz, DMSO-$d_6$) $\delta$ 3.37 (s, 4H), 3.67 (s, 6H), 3.81 (s, 12H), 4.13 (s, 4H), 7.01 (s, 4H), 9.89 (s, 4H); MS (EI) *m/z*: 420, [$M^{+\bullet}$], 181, $[(MeO)_3 - C_7H_4]^+$.

**(c)** *N,N′*-Bis(3,4,5-trimethoxybenzyl)ethylenediamine *N,N′*-diacetic acid dihydrochloride (**L1**) was obtained from the corresponding diamine (14.0 g, 28.4 mmol) according to the general procedure. The crude product was recrystallized from ethanol/water 1:1 to yield 10.6 g (60%) of the pure compound as a white powder: mp 205 °C; $^1$H NMR (500 MHz, DMSO-$d_6$) $\delta$ 2.82 (s, 4H), 3.27 (s, 4H), 3.63 (s, 6H), 3.71 (s, 12H), 3.74 (s, 4H), 6.64 (s, 4H); MS (DCI($NH_3$)) *m/z* 537, $[M + H]^+$; 181, $[(MeO)_3 - C_7H_4]^+$. Anal. Calcd for $C_{26}H_{36}N_2O_{10}\cdot 2HCl$: C, 51.24; H, 6.28; N, 4.60; O, 26.25. Found: C, 51.67; H, 6.49; N, 4.60; O, 26.36.

***N,N′*-Dibenzylethylenediamine *N,N′*-Diacetic Acid (L2). (a)** *N,N′*-Dibenzylidene ethylenediamine was obtained according to the general procedure from benzaldehyde (35.0 g, 330 mmol) and ethylenediamine as a yellow oil (40 g, 100%) which was used without further purification for the next reaction step: $^1$H NMR (200 MHz, DMSO-$d_6$) $\delta$ 3.89 (s, 4H), 7.40−7.45 (m, 6H), 7.70−7.73 (m, 4H), 8.34 (s, 2H).

**(b)** *N,N′*-Dibenzylethylenediamine dihydrochloride was prepared according to the general procedure from the corresponding diimine (40.0 g, 169.0 mmol) as a white solid (26.6 g, 50%):$^1$H NMR (400 MHz, DMSO-$d_6$) $\delta$ 3.38 (s, 4H), 4.19 (s, 4H), 7.41−7.46 (m, 6H), 7.58−7.61 (m, 4H), 9.83 (s, 4H).

**(c)** *N,N′*-Dibenzylethylenediamine *N,N′*-diacetic acid (**L2**) was synthesized from the corresponding diamine (26.5 g, 84.6 mmol) according to the general procedure. The crude product was recrystallized from ethanol/water 1:1 to yield 21 g (69%) of the pure compound as a white powder: $^1$H NMR (400 MHz, DMSO-$d_6$) $\delta$ 2.76 (s, 4H), 3.22 (s, 4H), 3.74 (s, 4H), 7.24−7.32 (m, 10H), 12.0 (m, 2H); ESI/MS *m/z* 355 [M − H]$^-$. Anal. Calcd for $C_{20}H_{24}N_2O_4$: C, 67.39; H, 6.78; N, 7.86; O, 17.95. Found: C, 66.73; H, 6.73; N, 7.76; O, 17.94.

***N,N′*-Bis(3,4,5-trimethoxybenzyl)-1,3-diaminopropane *N,N′*-Diacetic Acid (L3). (a)** *N,N′*-Bis(3,4,5-trimethoxybenzylidene)-1,3-diaminopropane was obtained as a colorless oil with 100% yield according to the general procedure from 1,3-diaminopropane (1.0 g) and 3,4,5-trimethoxybenzaldehyde (5.0 g, 2.5 mmol). The compound was not characterized and used in the next reaction step without further purification.

**(b)** *N,N′*-Bis(3,4,5-trimethoxybenzyl)-1,3-diaminopropane dihydrochloride was obtained from the corresponding diimine (5.5 g, 13 mmol) according to the general procedure as a white solid (4.1 g, 63%): $^1$H NMR (200 MHz, DMSO-$d_6$) $\delta$ 2.90 (m, 2H), 2.99 (s, 4H), 3.66 (s, 6H), 3.80 (s, 12H), 4.04 (s, 4H), 7.02 (s, 4H), 9.64 (s, 4H).

**(c) *N,N′*-Bis(3,4,5-trimethoxybenzyl)-1,3-diaminopropane *N,N′*-diacetic acid (L3)** was obtained from the corresponding diamine (2.0 g, 3.9 mmol) according to the general procedure. The crude product was recrystallized from ethanol/water 1:1 to yield 0.7 g (30%) of the pure compound as a white powder: mp 204 °C; $^1$H NMR (500 MHz, DMSO-$d_6$) $\delta$ 1.65 (m, 2H), 2.66 (t, 4H), 3.21 (s, 4H), 3.63 (s, 6H), 3.70 (s, 4H), 3.72 (s, 12H), 6.61 (s, 4H). Anal. Calcd for $C_{27}H_{38}N_2O_{10}$: C, 58.90; H, 6.96; N, 5.09; O, 29.06. Found: C, 58.70; H, 6.98; N, 4.87; O, 29.24.

***N,N′*-Bis(3,4,5-trimethoxybenzyl)ethylenediamine *N,N′*-Dipropionic Acid (L4). (a) Ethylenediamine *N,N′*-Dipropionic Acid Diethyl Ester.** Thionyl chloride (3.9 g, 33 mmol) was added dropwise to a suspension of ethylenediamine *N,N′*-dipropionic acid (1.5 g, 7.5 mmol.) in 100 mL of dry ethanol. The mixture was heated at 75 °C for 24 h, filtered hot, and allowed to cool. The white precipitate was filtered, washed with cold ethanol, and dried. The crude product was recrystallized from ethanol to yield 1.2 g (31%) of the diester as a white powder: $^1$H NMR (400 MHz, DMSO-$d_6$) $\delta$ 1.2 (t, 6H), 2.80 (t, 4H), 3.20 (t, 4H), 3.32 (s, 4H), 4.12 (q, 4H), 9.55 (s, 4H).

**(b) *N,N′*-Bis(3,4,5-trimethoxybenzyl)ethylenediamine *N,N′*-Dipropionic Acid Diethyl Ester.** A mixture of 0.95 g (3.7 mmol) of ethylenediamine *N,N′*-dipropionic acid diethyl ester, 0.9 mL triethylamine, 0.75 g $CaCO_3$ and 1.6 g 3,4,5-trimethoxybenzyl chloride (7.4 mmol) in 40 mL DMF was heated to 80 °C for 4 h. The reaction mixture was evaporated to dryness, and 50 mL of water was added. Concentrated hydrochloric acid was used to adjust the pH to 1. The mixture was extracted with 2 × 100 mL of dichloromethane. The organic phase was washed with brine, dried ($Na_2SO_4$), and evaporated in vacuo. The residue was purified by chromatography on silica gel (eluant dichloromethane:methanol, 98:2) to yield 0.6 g (26%) of the pure compound as a colorless oil: $^1$H NMR (400 MHz, DMSO-$d_6$) $\delta$ 1.18 (t, 6H), 2.39 (t, 4H), 2.54 (s, 4H), 2.77 (t, 4H), 3.47 (s, 4H), 3.77 (s, 12H), 3.78 (s, 6H), 4.05 (q, 4H), 6.48 (s, 4H).

**(c) *N,N′*-Bis(3,4,5-trimethoxybenzyl)ethylenediamine *N,N′*-Dipropionic Acid (L4).** A mixture of 2.2 g (3.5 mmol) of *N,N′*-bis(3,4,5-trimethoxybenzyl)ethylenediamine *N,N′*-dipropionic acid diethyl ester in 40 mL of methanol and 20 mL of 1 M NaOH was stirred at room temperature for 2 h. The solvent was evaporated off, and 25 mL of water was added. The resulting solution was washed with 50 mL of dichloromethane, acidified with HCl (pH 4.5), and concentrated in vacuo. On cooling to 0 °C, a solid precipitated which was isolated by filtration, giving **L4** (0.20 g, 9%) as a white solid: mp 220 °C; $^1$H NMR (400 MHz, DMSO-$d_6$) $\delta$ 2.80 (s, 4H), 3.18 (s, 4H), 3.67 (s, 6H), 3.72 (s, 4H), 3.80 (s, 12H), 4.29 (s, 4H), 7.03 (s, 4H), 11.51 (s, 2H), 12.71 (s, 2H); ESI/MS *m/z* 563, [M − H]$^-$. Anal. Calcd for $C_{28}H_{40}N_2O_{10}\cdot 2HCl$: C, 52.75; H, 6.64; N, 4.39; O, 25.09. Found: C, 52.26; H, 6.48; N, 4.08; O, 25.33.

***N,N′*-Bis(3,4,5-trimethoxybenzyl)-1,2-diaminopropane *N,N′*-Diacetic Acid (L5). (a)** *N,N′*-Bis(3,4,5-trimethoxybenzylidene)-1,2-diaminopropane was obtained with 90% yield as a yellow solid according to the general procedure from 1,2-diaminopropane and 3,4,5-trimethoxybenzaldehyde (10.6 g, 40.0 mmol). It was directly used in the next reaction step.

**(b)** *N,N′*-Bis(3,4,5-trimethoxybenzyl)-1,2-diaminopropane dihydrochloride was obtained from the corresponding diimine (21.8 g, 50.6 mmol) according to the general procedure as a white solid (18.5 g, 72%): $^1$H NMR (200 MHz, DMSO-$d_6$) $\delta$ 1.64 (d, 3H), 3.45−3.60 (m,

3H), 3.82 (s, 6H), 3.96 (s, 12H), 4.17−4.30 (m, 4H), 7.23 (d, 4H), 10.15 (s, 4H).

**(c)** *N*,*N*′-Bis(3,4,5-trimethoxybenzyl)-1,2-diaminopropane *N*,*N*′-diacetic acid (**L5**) was obtained from the corresponding diamine (2.0 g, 3.9 mmol) according to the general procedure. The crude product was recrystallized from water to yield 1.65 g (67%) of the pure compound as a white powder: mp 144 °C; $^1$H NMR (400 MHz, DMSO-$d_6$) $\delta$ 1.22 (d, 3H), 3.05 (dd, 1H), 3.36 (dd, 1H), 3.58 (dd, 2H), 3.64 (s, 3H), 3.65 (s, 3H), 3.74 (s, 6H), 3.75 (s, 6H), 3.74−3.80 (m, 2H), 4.00 (m, 4H), 4.20 (d, 1H), 6.77 (s, 2H), 6.92 (s, 2H); DCI/MS ($NH_3$) *m*/*z* 549 $[M - H]^-$. Anal. Calcd for $C_{27}H_{38}N_2O_{10}\cdot 2HCl$: C, 52.01; H, 6.47; N, 4.49; O, 25.66. Found: C, 52.47; H, 6.41; N, 4.32; O, 25.46.

***N*,*N*′-Bis(pyridin-2-ylmethyl)-*N*,*N*′-bis(3,4,5-trimethoxybenzyl)-ethan-1,2-diamine (L6).** *N*,*N*′-Bis(3,4,5-trimethoxybenzyl)ethylenediamine dihydrochloride (2.0 g, mmol) obtained as described above was dissolved in 30 mL of water. NaOH (30% solution) was added until the pH of the solution was adjusted to 11. Thereafter, 2-picolyl chloride (1.35 g, mmol) in water (15 mL) was added dropwise. The reaction mixture was stirred at 40 °C for 4 h. Aqueous NaOH (30% solution) was used to maintain the pH of the solution in the range of 10−11 throughout. The mixture was extracted with dichloromethane and the organic phase was washed with brine, dried and evaporated. The oily residue was purified by chromatography on silica gel (eluant dichloromethane:methanol, 98:2) to yield **L6** as a white powder: mp 106 °C; $^1$H NMR (400 MHz, $CDCl_3$) $\delta$ 2.82 (s, 4H), 2.70 (s, 4H), 3.54 (s, 4H), 3.72 (s, 4H), 3.75 (s, 12H), 3.78 (s, 6H), 6.53 (s, 4H), 7.08 (m, 2H), 7.38 (d, 2H), 7.53 (m, 2H), 8.45 (m, 2H); CDI/MS ($NH_3$) *m*/*z* 603 $[M + H]^+$, 181 $[(MeO)_3 - C_7H_4]^+$. Anal. Calcd for $C_{34}H_{42}N_4O_6$: C, 67.75; H, 7.02; N, 9.30; O, 15.93. Found: C, 68.25; H, 7.14; N, 9.15; O, 16.13.

***N*-(3,5-dimethoxybenzyl)ethylenediamine *N*,*N*′,*N*′-Triacetic Acid (L7). (a) *N*-(3,5-Dimethoxybenzylidene)-*N*′-acetylethylenediamine.** A mixture of 75 g (452 mmol) of 3,5-dimethoxybenzaldehyde and 44 mL (452 mmol) of *N*-acetylethylenediamine in 500 mL of methanol was heated to 50 °C for 1 h. The solvent was evaporated off, and 300 mL of diethyl ether was added to the oily residue. After 30 min of stirring at 0 °C, a white precipitate was collected by filtration, washed with diethyl ether, and vacuum dried to yield 96 g (85%) of the Schiff base: mp 86 °C; $^1$H NMR (400 MHz, DMSO-$d_6$) $\delta$ 1.79 (s, 3H), 3.31 (q, 2H), 3.59 (m, 2H), 3.77 (s, 6H), 6.58 (t, 1H), 6.91 (d, 2H), 7.85 (t, 1H), 8.23 (s, 1H).

**(b) *N*-(3,5-Dimethoxybenzyl)-*N*′-acetylethylenediamine.** The Schiff base (96 g, 384 mmol) was dissolved in 300 mL of ethanol to which 18.2 g (480 mmol) of $NaBH_4$ was added portionwise. The reaction mixture was stirred at 50 °C for 2 h and then ice-cooled. HCl (6 N) was then slowly added to acidify the solution to pH 1. The white precipitate was collected by filtration and dissolved in 100 mL of water. The solution was basified with KOH (pH 10) and extracted with dichloromethane (8 × 200 mL). The organic phases were combined, dried ($Na_2SO_4$), and evaporated to dryness to yield the monoacetylated diamine as an oil (83 g, 86%): $^1$H NMR (400 MHz, DMSO-$d_6$) $\delta$ 1.79 (s, 3H), 2.53 (m, 3H), 3.13 (m, 2H), 3.63 (s, 2H), 3.72 (s, 6H), 6.34 (dd, 1H), 6.50 (d, 2H), 7.75 (t, 1H).

**(c) *N*-(3,5-Dimethoxybenzyl)ethylenediamine.** Monoacetylated diamine (19.2 g, 76 mmol) was heated to reflux for 8 h in 60 mL of 6 M HCl. The solution was cooled, basified with NaOH (pH 10), and extracted with 5 × 50 mL of dichloromethane. The organic phases were combined, washed with 50 mL of water, dried ($Na_2SO_4$), and evaporated to dryness yielding the diamine (19.5 g, 60%) as an oil: $^1$H NMR (400 MHz, DMSO-$d_6$) $\delta$ 1.98 (s, 2H), 2.49 (t, 2H), 2.60 (t, 2H), 3.62 (s, 2H), 3.72 (s, 6H), 6.34 (dd, 1H), 6.51 (d, 2H).

**(d) *N*-(3,5-Dimethoxybenzyl)ethylenediamine *N*,*N*′,*N*′-Triacetic Acid Tri-*tert*-butyl Ester.** To a solution of 5.2 g (25 mmol) of diamine in 60 mL of DMF were added dropwise 10.8 mL (75 mmol) of triethylamine and then 21.4 mL (150 mmol) of *tert*-butyl chloroacetate. The mixture was heated to 60 °C for 2 h and then cooled and filtered. The solvent was evaporated off, and the residual oil was solubilized in 100 mL of dichloromethane and washed with 1 M HCl (3 × 70 mL). The organic phase was dried ($Na_2SO_4$) and evaporated to dryness. To the residual oil was added 300 mL of diethyl ether. The mixture was stirred at 0 °C for 30 min. The resulting white precipitate was collected by filtration, washed with diethyl ether, and dried, yielding 10.2 g (75%) of the triester: $^1$H NMR (400 MHz, DMSO-$d_6$) $\delta$ 1.38 (s, 18H), 1.42 (s, 9H), 2.65 (t, 2H), 2.73 (t, 2H), 3.25 (s, 2H), 3.37 (s, 4H), 3.66 (s, 2H), 3.71 (s, 6H), 6.36 (dd, 1H), 6.47 (d, 2H).

**(e) *N*-(3,5-Dimethoxybenzyl)ethylenediamine *N*,*N*′,*N*′-Triacetic Acid (L7).** Triester (1.87 g, 3 mmol) was heated to reflux for 5 h in 100 mL of 1 M HCl. The solvent was evaporated off, yielding a white precipitate. This crude product was purified by stirring the solid at 0 °C for 30 min in 100 mL of ethanol:ethyl acetate 6:4. The white solid was collected by filtration, washed with ether, and vacuum dried over $P_2O_5$ yielding the triacid **L7** (1.34 g, 95%): $^1$H NMR (400 MHz, DMSO-$d_6$) $\delta$ 3.15 (t, 2H), 3.34 (t, 2H), 3.57 (s, 4H), 3.76 (s, 6H), 4.07 (s, 2H), 4.35 (s, 2H), 6.57 (dd, 1H), 6.71 (d, 2H); ESI/MS *m*/*z* 383 $[M - H]^-$. Anal. Calcd for $C_{17}H_{24}N_2O_8\cdot 2HCl\cdot 1H_2O$: C, 43.03; H, 5.90; N, 5.91; O, 30.30. Found: C, 42.68; H, 5.91; N, 5.72; O, 30.42.

The concentration of water in each sample for elemental analysis has been measured by the Karl Fisher method.

**Crystallization of Complex 1.** Complex **1** crystallized from a complex **2** solution. Such a solution has been obtained by mixing $Fe(ClO_4)_3$ (0.25 mmol) with a solution of **L1** (0.25 mmol) deprotonated by 2 equiv of triethylamine (0.5 mmol) in 20 mL of ethanol. The addition of water containing 10 equiv of acetate led to a green solution of complex **2** (final volume 25 mL). The slow evaporation of the reaction solution led to the deposition of red crystals of **1**.

**Preparation of [Fe(L′2)(OH$_2$)].** The ligand L′2 (resulting from the hydroxylation of the ligand **L2**) has been prepared as previously.[27] Crystalline powder of the title complex can be obtained by mixing 0.5 mmol of $Fe(ClO_4)_3$ with L′2 deprotonated by KOH (1 equiv) in 20 mL of water after allowing the solution to stand for 1 day. Anal. Calcd for $[Fe(C_{20}H_{22}N_2O_6)(H_2O)]\cdot 1.5H_2O$ (MW = 470.1): C, 51.10; H, 5.53; N, 5.96; Fe, 11.88. Found: C, 51.23; H, 5.43; N, 6.05; Fe, 12.00.

**X-ray Crystallography.** Crystallographic experimental details for complex **1** are given in Table 1. A dark red octahedral crystal of $[Fe_4O_2(C_{26}H_{34}N_2O_{10})_4]\cdot 10H_2O$ (**1**) was closed in a capillary tube and mounted on a nicollet XRD four circle diffractometer using a graphite crystal monochromator ($\lambda$(Mo K$\alpha$) = 0.710 73 Å); 5689 reflections were collected at 293 K in a range of $3° \le 2\theta \le 50°$ and were corrected for Lorentz and polarization effects but not for absorption ($\mu$ = 0.518 mm$^{-1}$), and 5666 independent reflections were used in the structural analysis. The structure was solved using an automatic Patterson procedure (SHELXS-86) [Sheldrick, G. M. *Acta Crystallogr*, *Sect. A* **1990**, *46*, 467] and refined againsts all $F^2$ (SHELXL-93) [Sheldrick, G. M. *SHELXL-93: Program for the Refinement of Crystal Structures*, University of Göttingen, Germany, 1993]. All non-hydrogen atoms were refined anisotropically. Hydrogen atoms were included in the refinement at calculated positions, riding on the carrier atoms, with isotropic thermal parameters ($U$(H) = 1.5$U_{eq}$(C) for the methyl hydrogen atoms and $U$(H) = 1.2$U_{eq}$(C) for the aromatic hydrogen atoms and methylene hydrogen atoms). The solvent molecules of water were refined with isotropic thermal parameters. Final cycle refinement including 382 parameters converged to $R(F)$ = 0.109 [for 2171 $F > 4\sigma(F)$], wR($F^2$) = 0.292, and goodness of fit $S$ = 1.152 for all 5666 $F^2$.

**Oxidation Reactions.** Two sets of experiments, which gave the same results, were performed. First, in a typical experiment, to 2 mL of a $CH_3CN$:$H_2O$ solution (1:1, v/v) of 0.2 mM of complex **1** (or 0.4 mM of complex **2**) was added 2 $\mu$L of $H_2O_2$ 3% (5 equiv) (dilution 1/10 in acetonitrile). The reaction was monitored spectrophotometrically at 560 nm for **1** over 1 h. In some cases, the addition of triethylamine (4 equiv, 2.5 $\mu$L of 1/10 diluted solution) or acetate (10 equiv, 6.5 $\mu$L of a 0.65 M NaOAc leading to formation of complex **2**) was effected before addition of the oxidant. Second, in a 50 mM acetate buffer (pH 5.4) 1 mM of $FeCl_3$, 1 mM **L1** was incubated with $H_2O_2$ (3−10 mM final concentration). For reductive activation of $O_2$ experiments under both of the above solvent conditions, 1 mL of 0.013 M ascorbate (32 equiv, 8 per iron (III)) was added to 1 mL of a 0.4 mM solution of complex **1**. In one experiment, the reaction was performed under argon.

**NMR Characterization of the Oxidized L1 Ligand (L′1).** After a typical oxidation experiment with complex **1** in $D_2O$ acetate buffer, excess dithionite was added under anaerobic conditions and the $^{13}$C and $^1$H NMR spectra of the solution were recorded. Under these conditions, the reduced iron was no longer bound to the oxidized ligand.

**Table 1.** Crystallographic Experimental Details for Complex **1**

I. Crystal Data

| | |
|---|---|
| formula: $[Fe_4(\mu\text{-}O)_2(C_{26}H_{34}N_2O_{10})_4]\cdot 10H_2O$ | linear abs factor ($\lambda$Mo K$\alpha$): $\mu = 0.518$ mm$^{-1}$ |
| fw: 2563.68 | morphology:octahedron, dark red |
| cryst syst: tetragonal | cryst dimens:0.20 × 0.20 × 0.30 mm |
| $a = 21.006(16)$ Å | space group: $I4_1/a$ |
| $b = 21.006(16)$ Å | $V = 13203(17)$ Å$^3$ |
| $c = 29.923(22)$ Å | $Z$ (units/cell) = 4 |
| cell params from 23 reflns | $D_x = 1.285$ g/cm$^3$ |
| $F(000) = 5384$ | $\theta = 10-15°$ |

II. Intensity Measurements

| | |
|---|---|
| temp: 293 K | data collection limits:$3° \le 2\theta \le 50°$ ($0 \le h \le 25$, $0 \le k \le 25$, $0 \le l \le 35$) |
| diffractometer:four circle Nicolet XRD | 5689 measd reflns |
| monochromator:graphite (220) | 3 standard reflns |
| radiation: $\lambda$(Mo K$\alpha$) = 0.71073 Å | 5666 indep reflns |
| scan mode: $\omega$ scan | monitored every 200 reflns |
| scan width: 1.2° | |

III. Structure Determination and Refinement

| | |
|---|---|
| solved by Patterson procedure | SHELXS-86 |
| refinement on $F^2$ | SHELXL-93 |
| $R(F) = 0.109$ [for 2171 $F > 4\sigma(F)$] | $(\Delta/\sigma)_{max} = 0.063$ |
| $wR(F^2) = 0.292$ | $\Delta\rho_{max} = 0.52$ eÅ$^{-3}$ |
| $S = 1.152$ | $\rho_{max} = -0.32$ eÅ$^{-3}$ |
| no. of reflns: 5666 | refined params: 382 |
| calcd weights: $w = 1/[s^2(F_o^2) + (0.035P)^2 + 221.077P]$, where $P = (F_o^2 + 2F_c^2)/3$ | |

For **L′1**: $^1$H NMR (400 MHz, $D_2O$) $\delta$ 3.4 (t, 2H), 3.45 (t, 2H), 3.62 (s, 2H), 3.66 (s, 2H), 3.68 (s, 3H), 3.72 (s, 3H), 3.75 (s, 3H), 3.78 (s, 6H), 3.785 (s, 3H), 4.14 (s, 2H), 6.755 (s, 1H), 6.765 (s, 2H); $^{13}$C NMR (400 MHz, $D_2O$) 105.4, 108.4, 108.8, 124.14, 135, 138.5, 140.7, 140.9, 143.4, 150.14.

**Conversion Kinetics.** Initial rates of **L1** oxidation were determined by monitoring the time dependent variation of the absorbance of the phenoxo-to-iron LMCT of complex **3**, during a period when less than 10% of the conversion was done, using an extinction coefficient of 1500 (see results section). Oxidation of **L1** was also monitored by ESI-MS. The solution was injected 3 min after $H_2O_2$ addition and every tenth minute for 2 h and analyzed in terms of relative intensities of $[Fe_2O(OAc)(\mathbf{L1})]^-$ ion in the negative mode and the positive ion of complex **3** $[Fe\mathbf{L1}' + H]^+$ in the positive mode.

**Labeling Experiments.** Two sets of experiments have been performed. First, to a 1 mM $CH_3CN$: $H_2{}^{18}O$ solution (1:1, v/v) of complex **1** containing 10 mM ammonium acetate, previously deaerated, was added ascorbic acid (10 equiv, diluted in $H_2{}^{18}O$) or $H_2O_2$ (3 equiv). Second, a 1 mM solution of complex **1** with 10 equiv of ammonium acetate was degassed with helium and stocked under argon. The addition of ascorbic acid was effected under argon, and $^{18}O_2$ was introduced. When the reaction was complete, the mixture was analyzed by mass spectrometry for the presence of $^{18}$O in the product.

**Spin-Trapping Experiments.** In a standard experiment 2 $\mu$L of 5,5-dimethylpyrroline 1-oxide (DMPO) per milliliter of reaction solution was added before addition of $H_2O_2$. A multiplet EPR signal was obtained at 100 K corresponding to the hydroxyl adduct (DMPO−OH), only observed in the control experiment when complex **1** was replaced by the ferrous ion from Mohr's salt at identical concentration.

## Results

**1. Design and Synthesis of Diiron Complexes.** We have synthesized a series of EDTA analogues (**L1**−**L7**, Figure 1) and analyzed their ability to generate $\mu$-oxo dinuclear complexes with an acetate bridge during their reaction with iron salts in acetate buffer or in a water:acetonitrile (1:1) medium in the presence of acetate. As we intended to perform oxidation reactions in aqueous solutions exclusively, we used these media also for the preparation of the complexes. Consequently, we did not try to optimize their synthesis by using pure organic solvents and thus limited this study to the diiron complexes which could be generated under these specific conditions. The formation of such complexes has been concluded from (i) the presence of oxo-to-iron charge-transfer bands in the visible spectrum; (ii) ESI-MS analysis of the solution; (iii) the absence of an EPR signal; (iv) the characteristic $^1$H NMR spectrum with resonances spanning from 0 to 40 ppm.[1c,20] The two last properties reflect that the ferric ions are strongly antiferromagnetically coupled.

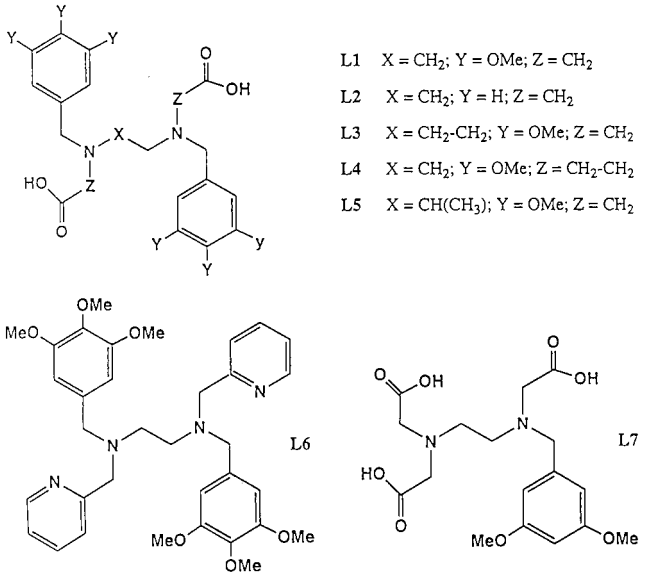


**Figure 1.** Structure of the ligands **L*n***.

As a result, we have observed that **L1**, **L2**, **L5**, and **L6** led to the formation of a $[Fe_2O(\mathbf{Ln})_2(OAc)]^+$ complex ($n$ = 1, 2, 5, 6). On the contrary, with **L3** and **L4**, containing an additional carbon in the diamine chain and the glycinyl chain, respectively, no evidence for such a complex could be obtained. Finally, **L7** led to a mixture of a mononuclear and dinuclear complexes as shown by ESI-MS.

Only in the case of **L1**, red crystals could be obtained from an ethanol:$H_2O$ mixture (v:v 5:1) of complex **2** allowed to stand for 2 days. The crystallized complex, noted **1**, was found to be a tetranuclear species as a result of the association of two

(20) Kurtz, D. M. *Chem. Rev.* **1990**, *90*, 585.

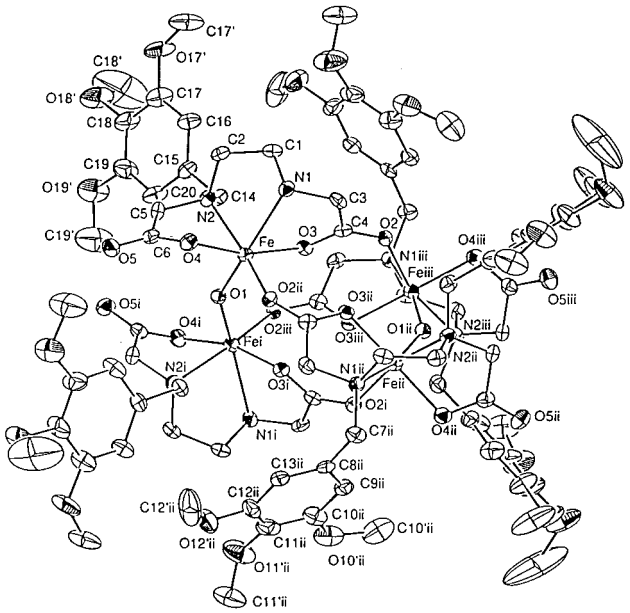


**Figure 2.** ORTEP representation of complex **1**. The benzyl moieties on N1 and N1i and hydrogen atoms have been omitted for clarity (see Supporting Information).

dinuclear **L1**Fe−O−Fe**L1** units. Spectroscopic analysis of the crystals revealed that the acetato bridge was no longer present in the complex. The full characterization of **1** has been carried out, and **1** has been considered as the prototype for other comparable systems from related ligands **L2**−**L7**.

**2. Structural Characterization of $Fe_4O_2(L1)_2$ (1).** The crystal structure of complex **1** (Figure 2) consists of a packing of discrete tetranuclear units $Fe_4(O)_2(\mathbf{L1})_4$ which are generated by a −4 axis (the $\mu$ oxygen O1 is located on the −4 axis). The tetranuclear core is built up by two $\mu$-oxo diiron(III) units (**L1**Fe−O−Fe**L1**) connected together by four equivalent carboxylate bridges (O2O3C4C5) belonging to different **L1** ligands. This arrangement leads to an iron core representing a tetrahedron with two short edges (3.389 Å) (iron connected by an oxo bridge) and four long edges (5.223 Å) (iron connected by a carboxylate bridge). The iron atoms are in an octahedral coordination, achieved by two nitrogen (N1,N2) atoms and two oxygen (O3,O4) atoms of a carboxylate group provided by one **L1** ligand, one oxygen atom from the oxo bridge and one oxygen atom O2 provided by a carboxylate moiety of another **L1** ligand. Structural parameters of the $Fe_2O(\mathbf{L1})_2$ unit are in the range of the well documented $\mu$-oxo diiron complexes with a short Fe−Ooxo distance of 1.7884(4) Å (Table 2). The Fe−O−Fe angle is in the low range for monobridged $\mu$-oxo diferric complexes, probably reflecting the constraints afforded by the two carboxylate bridge moieties (142.7°). As a consequence, the Fe···Fe distance is quite short [3.339 Å]. The $Fe-O_{carb}$ distances spread out between 2.014(8) and 2.039(8) Å, the shortest being with the oxygen atom (O4) of the carboxylate moieties of **L1**. Bridging bidentate carboxylate exclusively binds to iron through a trans coordination mode, as it has been observed in polynuclear ferrous complexes.[21] Monodentate carboxylates only use the anti lone pair of the oxygen atom O4. The anti coordination mode of the oxygen atom is generally observed in iron complexes containing a ligand with a glycinyl moiety and has been explained by constraints generated by the nitrogen binding. The two trimethoxybenzyl moieties of **L1** have

**Table 2.** Selected Bond Lengths (Å) and Angles (deg) for **1**[a]

| | | | |
|---|---|---|---|
| Fe···Fei | 3.389(4) | O1−Fei | 1.788(4) |
| Fe···Feii | 5.253(5) | O2−Feiii | 2.028(8) |
| Fe···Feiii | 5.253(5) | Fe−O3 | 2.039(8) |
| Fe−O1 | 1.788(4) | Fe−N2 | 2.209(10) |
| Fe−O4 | 2.014(8) | Fe−N1 | 2.331(10) |
| Fe−O2ii | 2.028(8) | | |
| O1−Fe−O4 | 98.4(4) | O1−Fe−N2 | 88.9(3) |
| O1−Fe−O2ii | 97.6(3) | O4−Fe−N2 | 77.4(3) |
| O4−Fe−O2 | 88.7(3) | O2ii−Fe−N2 | 165.4(3) |
| O1−Fe−O3 | 93.3(3) | O3−Fe−N2 | 93.0(3) |
| O4−Fe−O3 | 164.7(3) | O1−Fe−N1 | 162.7 |
| O2ii−Fe−O3 | 99.6 | O4−Fe−N1 | 92.9(3) |
| O2ii−Fe−N1 | 95.6(3) | Fe−O1−Fei | 142.7(7) |
| O3−Fe−N1 | 73.6(3) | N2−Fe−N1 | 80.9(4) |

[a] The estimated standard deviations are indicated in parentheses. Symmetry equivalent positions: (i) $1-x$, $^1/_2-y$, $z$; (ii) $^1/_4+y$, $^3/_4-x$, $^3/_4-z$; (iii) $^3/_4-y$, $x-{}^1/_4$, $^3/_4-z$.

two different orientations regarding the iron atoms. One lies far away from the tetranuclear unit, and the second is quite close to the Fe−O−Fe unit [Fe−C20 and C16 = 5.423 and 5.24 Å versus Fe−C13 and Fe−C9 = 3.852 and 5.03 Å, respectively].

The tetranuclear structure is quite unique. So far, such clusters consisting in the association of two dinuclear units were obtained via hydroxo/oxo (formed by hydrolytic reaction) and not carboxylato bridges.[22] This represents a new example of the binding versatility of carboxylates.

**3. Spectroscopic Studies and Solution Chemistry of Complex 1.** Complex **1** remained intact in solution when its crystals were solubilized in pure acetonitrile as shown by ESI-MS with a molecular peak at *m*/*z* 2392.6 (100) and the expected isotopic pattern for $[Fe_4O_2(\mathbf{L1})_4 + H]^+$ in the positive mode (Figure 3, Table 3). The UV−vis spectrum displayed three transitions at 560 ($\epsilon$ = 0.25 mM $cm^{-1}$), 370 (10), and 310 (15) nm (Table 4). These features are correlated to the presence of an oxo bridge between two ferric ions and have been attributed to oxo-to-iron(III) charge-transfer bands.[20,23] The presence of the magnetic interactions between the metal ions has been deduced from the absence of any EPR signal. The presence of broad resonances at 43.7, 26, 16, and 7 ppm in the $^1$H NMR, tentatively assigned to the methylene protons of the glycinyl and the diamine moieties of **L1**, is in agreement with a large antiferromagnetic spin coupling ($|J| > 90$ $cm^{-1}$).[20]

On the contrary, when complex **1** was solubilized in an acetonitrile:water solution (1:1, v/v), the tetranuclear core was slowly broken down into a $\mu$-oxo-diferric species with completion of the reaction occurring after 2 h. The same reaction was accelerated in the presence of 4 equiv of triethylamine. Accordingly, the ESI-MS spectrum showed that the tetranuclear ion has disappeared to be replaced by ions at *m*/*z* 1219(100) attributed to $[Fe_2O(L_1)_2 + Na]^+$ (Figure 4). The ligand on the sixth position on each iron coordination sphere is filled by a labile ligand, i.e., water or acetonitrile. The electronic and the $^1$H NMR spectra were similar to the ones of $[Fe_4O_2(\mathbf{L1})_4]$ (**1**) suggesting that the coordination mode of **L1** is not affected by the core structural changes.

Both in pure acetonitrile or in acetonitrile:water mixtures, addition of a variety of carboxylate anions (acetate, benzoate,

(21) (a) Ménage, S.; Fuji, H.; Hendrich, M. P.; Que, L., Jr. *Angew. Chem., Int. Ed. Engl.* **1994**, *33*, 1660. (b) Rardin, R. L.; Tolman, W. B.; Lippard, S. J. *New J. Chem.* **1991**, *15*, 417.

(22) (a) Hagen, K. S. *Angew. Chem., Int. Ed. Engl.* **1992**, *31*, 1010 and references therein. (b) Murch, B. P.; Bradley, F. C.; Boyle, P. D.; Papaefthymiou, V.; Que, L., Jr. *J. Am. Chem. Soc.* **1987**, *109*, 7993. (c) Drueke, S.; Wieghardt, K.; Nuber, B.; Weiss, J.; Bominaar, E. L.; Sawaryn, A.; Winkler, H.; Trautwein, A. X. *Inorg. Chem.* **1989**, *28*, 4477. (d) Sessler, J. L.; Sibert, J. W.; Burell, A. K.; Lynch, V.; Market, J. T.; Wooten, C. L. *Inorg. Chem.* **1993**, *32*, 4277.

(23) Ménage, S.; Que, L., Jr. *New J. Chem.* **1990**, *15*, 431.

**Table 3.** ESI-MS of Complexes with **L*n*** Ligands and Their Oxidized Forms after $H_2O_2$ or $O_2$/Ascorbate Oxidation

| Fe/**L*n*** complex | medium | ions *m*/*z* (%int) | attribution |
|---|---|---|---|
| **1** | $CH_3CN$ | 2392.6 (100) | $[Fe_4O_2(\mathbf{L1})_4 + H]^+$ |
| **1** | $CH_3CN$:$H_2O$ | 1219(100) | $[Fe_2O(\mathbf{L1})_2 + Na]^+$ |
| | | 1213 | $[Fe_2O(\mathbf{L1})_2 + OH]^-$ |
| **1** + OAc (**2**)[a] | $CH_3CN$:$H_2O$ or acetate buffer | 1255.5(100) | $[Fe_2O(\mathbf{L1})_2(OAc)]^-$ |
| | | 1257.3 (100) | $[Fe_2O(\mathbf{L1})_2(OAc) + 2H]^+$ |
| Fe/**L5** | $CH_3CN$:$H_2O$ | 1283.4 (30) | $[Fe_2O(\mathbf{L1})_2(OAc)]^-$ |
| Fe/**L6** | $CH_3CN$ | 745 (50) | $[Fe_2O(\mathbf{L6})_2(OAc)ClO_4]^{2+}$ |
| Fe/**L7** | $CH_3CN$:$H_2O$ | 438 (60) | $[Fe(\mathbf{L7}) + H]^+$ |
| | | 893 (30) | $[Fe_2O(\mathbf{L7})_2 + H]^+$ |
| | | 496 (60) | $[Fe(\mathbf{L7}) + OAc]^-$ |
| | | 472 (40) | $[Fe(\mathbf{L7}) + Cl]^-$ |
| | | 891 (50) | $[Fe_2O(\mathbf{L7})_2 - H]^-$ |
| **2** + Asc[b] | $CH_3CN$:$H_2O$ under Argon | 591 (100) | $[Fe^{II}(\mathbf{L1}) + H]^+$ |
| | | 625 (100) | $[Fe^{II}(\mathbf{L1}) + Cl]^-$ |
| | | 765 (100) | $[Fe^{II}(\mathbf{L1}) + asc]^-$ |
| | Oxidation Products | | |
| **2** + Asc[b]/$16O_2$ (**3**) | | 606 (100) | $[Fe(^{16}\mathbf{L'1})^c + H]^+$ |
| **2** + Asc/$^{18}O_2$ (**3**) | | 608 (100) | $[Fe(^{18}\mathbf{L'1}) + H]^+$ |
| **2** + $H_2O_2$ (**3**) | $CH_3CN$:$H_2O$ | 628 (80) | $[Fe(\mathbf{L'1}) + Na]^+$ |
| | | 606 (100) | $[Fe(\mathbf{L'1}) + H]^+$ |
| Fe(**L'2**)($H_2O$) | $CH_3CN$:$H_2O$ | 448 (50) | $[Fe(\mathbf{L'2}) + Na]^+$ |
| | | 426 (100) | $[Fe(\mathbf{L'2}) + H]^+$ |
| | | 442 (100) | $[Fe(\mathbf{L'2}) + OH]^-$ |
| | | 470 (60) | $[Fe(\mathbf{L'2}) + HCO_2]^-$ |

[a] Fe/**L*n*** corresponds to the mixture of $FeCl_3$ and **L*n*** in an acetate buffer (pH = 5.4). [b] OAc = acetate anion; Asc, ascorbate anion. [c] $^{16}$**L'1** refers to the 16O atom incorporated in **L1**.

**Table 4.** Spectroscopic Characteristics of Iron and **L1**−**L7** Complexes and Their Oxidized Analogs

| complex Fe/**L*n*** | $\lambda$ nm ($\epsilon$ $mM^{-1}\cdot cm^{-1}$) | | | | assignment |
|---|---|---|---|---|---|
| **1**[a] | 560 (0.25) | 370 (10) | 310 (15) | | LMCT $O_{oxo} \rightarrow Fe$ |
| **2**[a] | 640 (0.2) | 495(0.5) | 435(1.2) | 350(sh), 325(10) | |
| $[Fe_2O(\mathbf{L2})_2(OAc)]^-$ [a] | 640 (0.16) | 493(0.5) | 435(1.2) | 360(sh), 340(11.2) | |
| $[Fe_2O(\mathbf{L5})_2]$[b] | 640 (0.12) | 490(sh) | 430(sh) | 350(sh), 320(10.2) | |
| $[Fe_2O(\mathbf{L6})_2(OAc)]^{3+}$ [a] | 675 (0.2) | 515(0.5) | 470(1.5) | 360(sh), 325(10.5) | |
| [Fe(**L1'**)($H_2O$)](**3**)[b] | | 560 (1.5) | | | LMCT $O_{Ph} \rightarrow Fe$ |
| [Fe(**L2'**)($H_2O$)][b] | | 526 (1.5) | | | |
| [Fe(**L5'**)($H_2O$)][b] | | 570 (nd) | | | |
| [Fe(**L7'**)($H_2O$)][b] | | 590 (nd) | | | |

[a] $CH_3CN$:$H_2O$ (1:1). [b] Acetate buffer 50 mM (pH = 5.4). **L'*n*** corresponds to the monohydroxylated analogue of **L*n***.

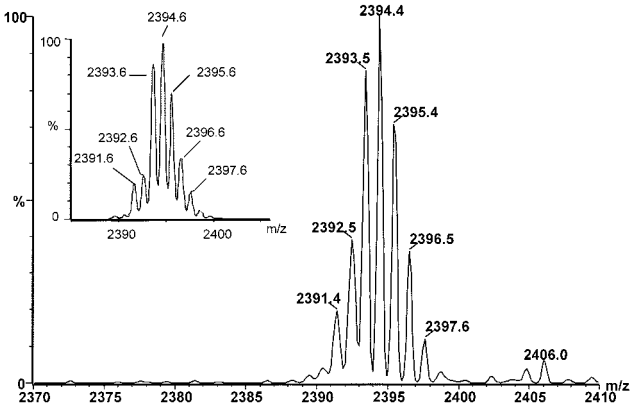


**Figure 3.** MaxEnt reconstruction spectrum (ESI$^+$, 49 iterations) of complex **1** in acetonitrile as well as a comparison of the peak envelope around 2393.5 to the theoritical isotopic distribution of the pseudomolecular ion $[C_{104}H_{136}Fe_4N_8O_{42} + H]^+$ (inset).

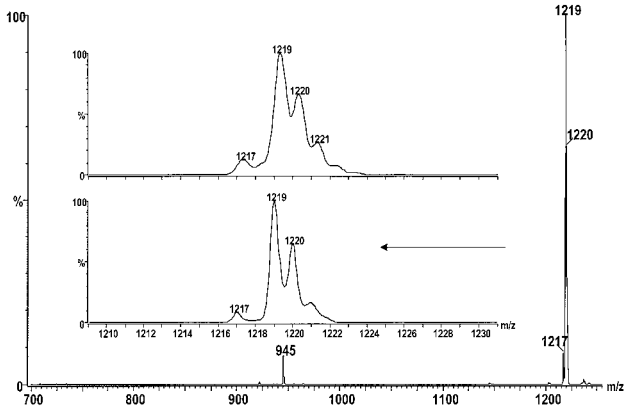


**Figure 4.** MaxEnt reconstruction spectrum (ESI$^+$, 26 iterations) of complex **1** in acetonitrile: water 1:1 as well as a comparison of the peak envelope at 1219 to the theoritical isotopic distribution of the pseudomolecular ion $[C_{52}H_{68}Fe_2N_4O_{21} + Na]^+$ (inset).

propionate and chloroacetate) converted complex **1** into a $\mu$-oxo $\mu$-carboxylato diferric complex, noted complex **2** in the case of acetate. For example, the ESI-MS spectrum of a solution of complex **1** with 10 equiv of acetate presented only one major peak at *m*/*z* 1255.5 (100) corresponding to the $[Fe_2O(\mathbf{L1})_2(OAc)]^-$ ion in the negative mode, 1257.3 (100) and 1279.2 expected for the fragments $[Fe_2O(\mathbf{L1})_2(OAc) + 2H]^+$ and $[Fe_2O(\mathbf{L1})_2$-$(OAc) + Na + H]^+$, respectively (Table 3). The MS/MS experiments on the *m*/*z* 1255 fragment revealed the loss of *m*/*z* 60 fragment, demonstrating the presence of an acetate anion in the parent ion. The addition of acetate to a $CH_3CN$:$H_2O$ solution of complex **1** also caused a drastic change of the UV−vis spectrum, with the appearance of new transitions at 640 (0.2 mM $cm^{-1}$), 495 (0.5), 435 (1.2), 350 (sh), and 325 (10) nm.

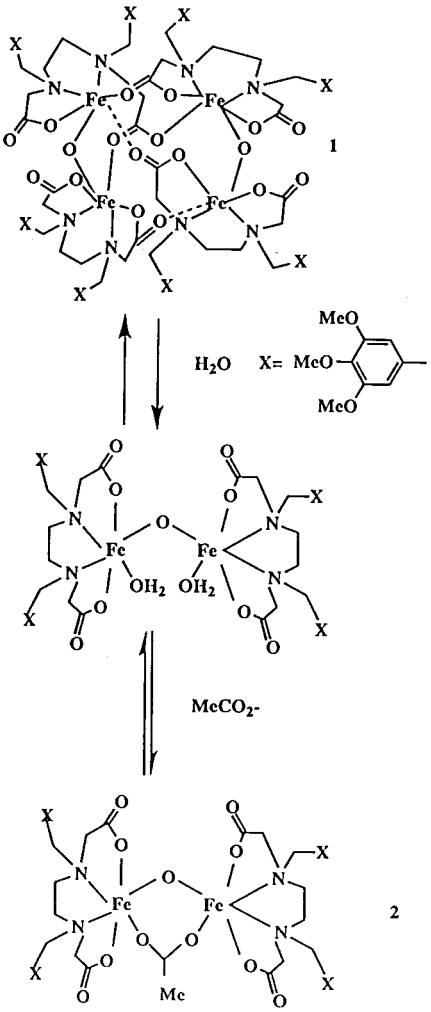


**Figure 5.** Schematic representation of the three species present in a $CH_3CN$:$H_2O$ solution of complex **1** in the presence of acetate.

Such transitions were in agreement with the presence of an additional acetato bridge.[20,23] Accordingly, the low-energy transition in the visible region (forbidden oxo-to-iron LMCT) shifted by 20 nm when acetate was replaced by other carboxylate anions. When laser excited at 406.7 nm, the acetate-buffered **2** solution (pH = 5.4) exhibited a resonance enhanced Raman feature at 505 $cm^{-1}$. This resonance, attributed to the $\nu_s$ Fe−O−Fe, is in the range of those for structurally characterized $\mu$-oxo $\mu$-carboxylato diiron complexes.[24] From the Sanders−Loehr correlation, an angle of 130° can be proposed for complex **2**. The coordination mode of the carboxylate could be also assessed by $^1$H NMR: the presence of the methyl resonance of the acetato anion at 12.5 ppm further confirmed its bidentate bridging coordination mode.[25] This was also true with the other carboxylate anions ($\delta$ $CH_2$ = 11.3, propionate; $\delta$ *m*-Obz = 9.03, benzoate bridge). The excess of acetate required for a complete transformation of **1** into **2** was solvent dependent. In particular, when $H_2O$ was present in the reaction medium higher equivalents of acetate were needed. This reflected the competition between water and the labile carboxylate anion for coordination to iron.

In water:acetonitrile solution containing acetate, at least three species are then in equilibrium, as depicted in Figure 5. As complex **1** gives rise to a dinuclear $\mu$-oxo complex during reaction with water, as shown by ESI-MS, we propose that water molecules are present in the complex as labile sixth ligand (Figure 5). This equilibrium may explain our difficulties to isolate complex **2** in a crystalline pure form, as the selective formation of crystals of complex **1** continuously shifted the equilibrium to **1** during crystallization.

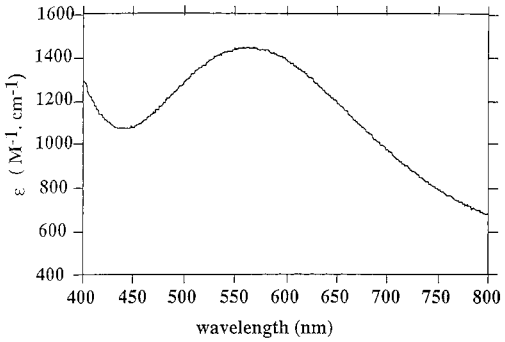


**Figure 6.** UV−vis spectrum of complex **3**.

**4. Characterization of Diiron(III) Complexes with L*n* Ligands.** The introduction of a pyridine in place of carboxylate moieties (ligand **L6**) led to a complex whose spectroscopic properties in $CH_3CN$:$H_2O$ medium were in agreement with its description as a $\mu$-oxo $\mu$-acetato diiron(III) complex, $[Fe_2O(OAc)(\mathbf{L6})_2](ClO_4)_3$. Accordingly, the oxo-to-iron(III) LMCTs were red shifted compared to those of complex **2** (Table 4) and proton resonances of the pyridine hydrogen atoms at 36 (*o*-Hpyr or $CH_2$), 23 (*o*-Hpyr or $CH_2$), 16.6 (*m*-Hpyr), and 6.5 (*p*-Hpyr) ppm and 15 ppm for the methyl group of the carboxylate could be attributed according to $^1$H NMR of related complexes.[26] Furthermore, the ESI-MS spectrum contains a peak at $m/z$ = 745 corresponding to the fragment $[Fe_2O(OAc)(\mathbf{L6})_2(ClO_4)]^{2+}$, as proved by the similarity of its isotopic pattern with a theoritical one. In the case of **L2** and **L5**, a $\mu$-oxo $\mu$-acetato complex has also been obtained in $CH_3CN$:$H_2O$ in the presence of acetate or in acetate buffer pH = 5.4 as shown by ESI-MS (Table 3). Both complexes gave rise to an UV−vis spectrum identical to the one of complex **2** (Table 4). **L7** afforded a mixture of mononuclear and $\mu$-oxo dinuclear complexes as revealed by ESI-MS. From ESI-MS, it was also clear that the dinuclear unit was not acetato bridged (see Table 3). Accordingly, no defined features could be observed in the visible spectrum.

**5. Reductive Activation of $O_2$ by Complex 1.** Under conditions in which **1** is converted to **2**, i.e., in an aerated $CH_3CN$:$H_2O$ solution containing an excess of acetate or in acetate buffer pH = 5.4, addition of 10−20 equiv of ascorbate led to a new complex, noted **3**, with a new chromophore characterized by a strong absorption at 560 nm (Figure 6). The rate of complex **3** formation was dependent on ascorbate concentration. The reaction also proceeded with dithiothreitol or glutathione, albeit at much slower rates and yields (20% in the case of dithiothreitol). The presence of acetate was not absolutely required for the conversion of **1** into **3**.

Complex **3** was extracted from the reaction solution with $CH_2Cl_2$ after 1 h, dried, and analyzed by ESI-MS and EPR. ESI-MS indicated that **3** was a mononuclear species with a molecular mass corresponding to one ligand (**L1**), one iron, and one additional oxygen atom (Table 3 and Figure 7a). This was also confirmed from its EPR spectrum which displayed a signal centered at $g$ = 4.3, corresponding to a mononuclear high-spin

(24) Sanders-Loehr, J.; Wheeler, W. D.; Shiemke, A. K.; Averill, B. A.; Loehr, T. M. *J. Am. Chem. Soc.* **1989**, *111*, 8084.

(25) Arafa, I. M.; Goff, H. M.; David, S. S.; Murch, B. P.; Que, L., Jr. *Inorg. Chem.* **1987**, *26*, 2779.

(26) (a) Ménage, S.; Vincent, J.-M.; Lambeaux, C.; Chottard, G.; Grand, A.; Fontecave, M. *Inorg. Chem.* **1993**, *32*, 4766 and references therein.

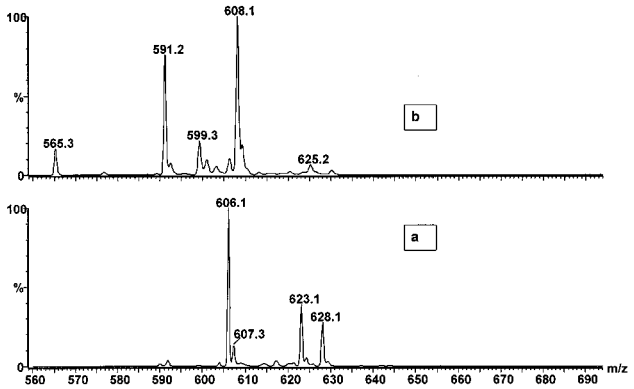


**Figure 7.** $ESI^+$-MS spectra obtained during the oxidation of complex **1**, in the presence of ascorbic acid and ammonium acetate: ($V_c$ = 35 V) with air $CH_3CN/H_2{}^{18}O$ (a) or $^{18}O_2$ in a $CH_3CN/H_2O$ solution (b). The detection of the ion at *m*/*z* 591.4 shows that the reaction in the presence of $^{18}O_2$ was incomplete. This ion corresponds to the pseudomolecular ion of the mononuclear ferrous complex.

ferric ion. The EPR signal intensity was directly correlated to the absorbance of the new chromophore. To confirm the oxidative attack of the ligand, the reaction mixture, after 1 h reaction, was treated by an excess of EDTA at 60 °C in order to demetalate the complex and then analyzed by HPLC/ESI/MS. Only 5% of the starting ligand was found unreacted. The major product (80% yield) was identified as the full ligand hydroxylated on a single phenyl group, based on fragmentation properties. The chromatogram also showed very minor products some of which were identified as trimethoxy benzaldehyde, resulting mainly from oxidation at $CH_2$ positions and cleavage.[27] The incorporation of the oxygen atom exclusively into the phenyl group was confirmed by FAB and in FAB/MS/MS. The fragmentation of the pseudomolecular peak in positive mode of complex **3** has confirmed the position of the oxygen atom in ortho position of the aromatic ring by the loss of a neutral fragment $C_{10}H_{12}O_4$ (*m*/*z* 196 for $^{16}O$ fragments), attributed to 2,3,4-trimethoxy-6-methylenecyclohexa-2,4-dienone.

$^1H$ and $^{13}C$ NMR spectra of the anaerobically dithionite reduced complex **3** have been recorded (see Experimental Section). The comparison of these spectra with that of the starting **L1** ligand confirmed that the ligand has been hydroxylated at the ortho position of the phenyl ring. As a matter fact, the 6.64 ppm resonance corresponding to the four *o*-hydrogen atoms in the **L1** spectrum has been replaced by two resonances at 6.75 (1H) and 6.76 ppm (2H), accounting for three hydrogen atoms only. This attests that only one *o*-hydrogen atom of the two phenyl groups of **L1** has been oxidized.

Even though no crystal structure for **3** could be obtained, all of these data unambiguously show that the reaction consists of a monohydroxylation of **L1**. The reaction is metal dependent since no oxidation of **L1** occurred in the absence of iron. The resulting phenol binds to iron leading to a strong phenoxo-to-iron charge-transfer band at 560 nm. Complex **3** is then formulated as [Fe**L′1**($H_2O$)] (see Scheme 1), **L′1** being *N*-(2-hydroxy-3,4,5-trimethoxybenzyl)-*N*′-(3,4,5-trimethoxybenzyl)-ethylenediamine *N*,*N*′-diacetic acid. The extinction coefficient of the LMCT, estimated from the amount of ligand recovered after reaction at pH = 5.4 was found equal to 1500 M $cm^{-1}$. Such a value is in the range of the extinction coefficients measured for other mononuclear phenolato ferric complexes (1200−4500).[28]

To dissect the reaction into a reducing step and an oxidation step, complex **1** was first anaerobically incubated with ascorbate. The reduction was monitored spectroscopically from the bleaching of the solution, due to the loss of the absorptions between 300 and 800 nm. The solution was also analyzed by ESI-MS which unambiguously showed the presence of a mononuclear ferrous complex (Table 3). The ESI-MS spectrum displayed molecular ions at *m*/*z* 591, 625, and 765 attributed to $[Fe^{II}(\mathbf{L1}) + H]^+$, $[Fe^{II}(\mathbf{L1}) + Cl]^-$ and $[Fe^{II}(\mathbf{L1}) + \text{ascorbate}]^-$ respectively (data not shown; some of these peaks are observed in Figure 7a). The $^1H$ NMR spectrum of the reduced complex, with two broad resonances at 85 and 40 ppm, tentatively assigned to the two kinds of methylene protons ligated to a high spin ferrous ion, was similar to that of an equimolar mixture of ferrous ion and **L1** (in the absence of ascorbate) under anaerobiosis. This further confirms the 1:1 $Fe^{II}$:**L1** stoichiometry in the reduced complex.

Addition of air to the ascorbate reduced complex **1** solution almost instantaneously led to the appearance of the stable blue chromophore, characteristic of complex **3**. Such a result was obtained also by admitting air into an anaerobic equimolar $Fe^{II}$:**L1** solution in the absence of ascorbate but the kinetic of this reaction was found slower than that one obtained in the presence of reductant. Accordingly, addition of ascorbate to the ferrous solution greatly accelerated the air-dependent formation of complex **3**.

An aromatic hydroxylation was also effective in the case of **L2**, **L5**, and **L7** as shown by the appearance of LMCT bands between 526 and 590 nm (Table 4) (**L′*n*** refers to the monohydroxylated ligand $\mathbf{L}_n$ in the text and tables). In the case of **L2**, this was further confirmed by ESI-MS (Table 3). In the case of **L6**, the destruction of the $\mu$-oxo diferric complex was observed, as shown by the bleaching of the solution but no chromophore was built up.

In the case of **L2**, the hydroxylated ligand was synthesized and served to prepare the iron complex [Fe**L′2**($H_2O$)], with satisfactory elemental analysis, which was fully characterized (see Tables 3 and 4). Its UV−vis spectrum displayed the expected phenoxo to iron(III) CT band. The presence of water as the sixth ligand was consistent with acid base titration experiments with this complex. They showed a reversible pH-dependent shift of the LMCT maximum energy, from 526 to 480 nm, from which a p$K_a$ value for the Fe−$OH_2$/Fe−OH couple of 5.9 was calculated. All of the spectroscopic properties were identical to those of the complex generated during the reaction of $[Fe_2O(OAc)(\mathbf{L2})_2]^-$ with $O_2$ in the presence of ascorbate. The blue shift of the absorption band, compared to that of **L1**, is in agreement with the variation of the electron density of the phenol ligand, resulting from the absence of the methoxy groups (Table 4).

**Activation of $H_2O_2$ by Complex 2.** Complex **1** was stable in the presence of 5 equiv of $H_2O_2$ in pure acetonitrile. However, when **1** was converted into a dinuclear complex upon addition of water or acetate, hydroxylation of the ligand by hydrogen peroxide occurred. The dependence of the reaction rate on acetate concentration is shown in Figure 8. As it perfectly matched the dependence of the intensity of the absorption at 640 nm on acetate concentration, characteristic of the conversion of **1** into **2**, it is very likely that only the binuclear complex **2**

(27) Galey, J. B.; Dumats, J.; Génard, S.; Destrée, O.; Pichaud, P.; Catroux, P.; Marrot, L.; Beck, I.; Fernandes, B.; Barre, G.; Hussler, G.; Seité, M.; Hocquaux, M. *Biochem. Pharmacol.* **1996**, *51*, 103.

(28) For example, see: (a) Carrano, C. J.; Carrano, M. W.; Sharma, K.; Backes, G.; Sanders-Loehr, J. S. *Inorg. Chem*, **1990**, *29*, 1865 (b) Lever, A. B. P. *Inorganic Electronic Spectroscopy*; Elsevier: New York, 1984; p 311.

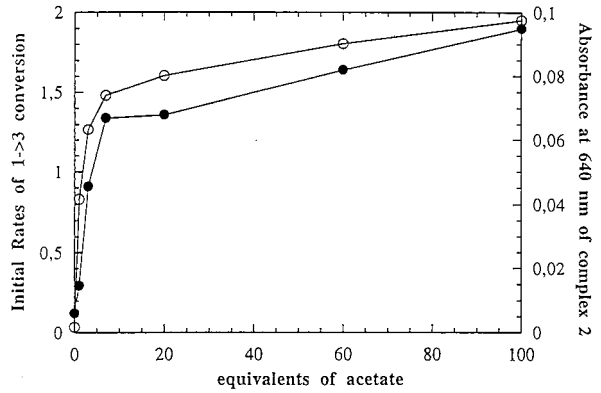


**Figure 8.** Initial rates (percent conversion $min^{-1}$) of the conversion **1** into **3** (○) and the concentration of complex **2**, calculated from the LMCT at 640 nm (●), as a function of acetate concentration. $[Fe_4O_2(\mathbf{L1})_4] = 0.25$ mM, $[H_2O_2] = 1.5$ mM.

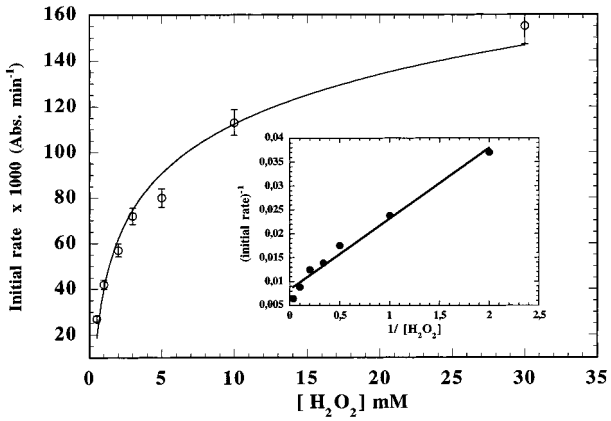


**Figure 9.** Initial rates for the formation of complex **3** as a function of hydrogen peroxide concentration. Inset: reciprocal plot of the initial rates versus $H_2O_2$ concentration. Experimental conditions: $[FeCl_3] = 1$ mM, $[\mathbf{L1}] = 1$ mM in 50 mM acetate buffer pH = 5.4. The errors on initial rates were estimated to 5% of the measured value; initial rates are measured as absorbance variation versus time.

and not its tetranuclear precursor was active during $H_2O_2$ activation. The conversion of **2** into **3** could be nicely monitored by ESI-MS from the parallel time-dependent increase of the $[Fe\mathbf{L'1} + H]^+$ ion at *m*/*z* 606 and the decrease of the $[Fe_2O(\mathbf{L1})_2(OAc)]^-$ at *m*/*z* 1255 ion peak (data not shown).

Complex **3** was stable in the presence of less than 10 equiv of $H_2O_2$. However, much larger excesses led to the loss of the chromophore and to an increase of the fragmented nonpolar products as showed by HPLC−mass spectrometry. The maximal yield during formation of **3** was thus obtained with 3 equiv of oxidant with regard to complex **2** concentration.

The reaction rate was also $H_2O_2$ concentration dependent. Kinetic experiments showed a saturation behavior with regard to $H_2O_2$ (Figure 9). At the very short reaction time selected, no decomposition of **3** could be observed. According to a Michaelis−Menten kinetic law, a linear correlation was observed in the plot of the reciprocals of initial rates versus reciprocals of hydrogen peroxide concentration (see the inset of Figure 9). A $K_m$ value of 0.56 mM was calculated. This strongly suggested the binding of the oxidant to complex **2** and may indicate that the resulting peroxo complex is a true reaction intermediate.

The reaction was general as the same aromatic oxidation (shown by ESI-MS and/or UV−vis spectroscopy) occurred with **L2**, **L5**, and **L7**, generating phenoxo to iron complexes, characterized by a LMCT band with comparable energy (Table 4). However, yields and rates were significantly lower as compared to that of **L1**. The reaction yield after 1 h at 37 °C, based on the assumption that the LMCT extinction coefficients were comparable for all the complexes, decreased as the following: **L1** (80%) > **L2** (60%) > **L5** (50%) ≫ **L7** (5%). It reached 70−80% after 48 h in the case of **L7**. Only in the case of **L6** was the dinuclear complex $[Fe_2O(OAc)(\mathbf{L6})_2](ClO_4)_3$ destroyed, but surprisingly no evidence for the phenolate complex could be obtained.

**Mechanistic Studies.** While both $H_2O_2$ and $O_2$/ascorbate oxidant systems were efficient to convert **1** into **3**, free $H_2O_2$ was not involved in the $O_2$/ascorbate system as addition of catalase had no inhibitory effects on the reaction.

To identify the source of the oxygen transferred to the ligand, oxidation of **1** was carried out with $^{18}O_2$ in the $O_2$/ascorbate system and with $H_2{}^{18}O$ in both the former and the $H_2O_2$ system. Complex **3** was analyzed by ESI-MS and was found to contain exclusively $^{18}O$ when $^{18}O_2$ was used as the oxidant and exclusively $^{16}O$ when $H_2{}^{18}O$ was used as the solvent (Table 2 and Figure 7b). $^{18}O$ incorporation has been further shown by FAB/MS analysis of the ligand of complex **3**, after in situ decomplexation by EDTA. The observation of the pseudomolecular ion at *m*/*z* at 553 $[M - H]^-$ is in total agreement with the labeled oxygen incorporation. There is no ambiguity that the phenol oxygen derives from the oxidant, exclusively.

When 30 equiv of $CBr_4$ was introduced in the reaction mixture, neither incorporation of Br atom into the ligand (ESI-MS) nor significant decrease of the yield of complex **3** was observed, even though the conversion rate was a bit lower than the control rate.

Addition of excess DMPO, a spin trapping agent,[29] into a $CH_3CN$:$H_2O$ solution of complex **1**/acetate either with $O_2$/ascorbate or $H_2O_2$ did not lead to the formation of the EPR active DMPO−OH radical, which results from the coupling between DMPO and hydroxyl radicals. A control reaction using $H_2O_2$ in which **1** has been replaced by ferrous ion has led to the observation by EPR of the DMPO−OH signal (Fenton reaction).

The conversion of **1** into **3** was not observed with alkylhydroperoxides or *m*-CPBA, but a low yield of **3** was obtained when PhIO (added as a solid) was used as an oxidant.

## Discussion

EDTA is a well-known ligand for iron. It has also proved to be efficient in stabilizing dinuclear ferric complexes in aqueous solution.[30] This was also the case for the original EDTA analogues that we synthesized to prepare water-stable diiron complexes, in which the coordination sphere is dominated by oxygen atoms as in the active site of the enzyme methane monooxygenase.[6b] Most of the previously reported catalytically active model complexes have diiron centers with an environment essentially made of nitrogen.[15] The replacement of two acetate moieties by benzyl moieties did not seriously affect the ability of the new ligands to generate dinuclear iron complexes.

The solution chemistry of nonheme iron is complex. In general, several oxo-bridged iron complexes with various nuclearities coexist in an equilibrium which may be controlled by organic ligands. The use of polynucleating ligands is an additional source of structural diversity. Furthermore, as is exemplified here, this complexity and the question of nuclearity

(29) Buttner, G. R. *Free Radical Biol. Med.* **1987**, *3*, 259.
(30) (a) Lippard, S. J.; Shugar, H. J.; Walling, C. *Inorg. Chem.* **1967**, *6*, 1825. (b) Motekaitis, R. J.; Martell, A. E.; Hayes, D.; Freiner, W. W. *Can. J. Chem.* **1980**, *58*, 1999.

may not be solved by X-ray crystallography if only one of the species in solution is prone to give rise to crystals. However, the formation of a dinuclear complex in solution can be unambiguously shown from a variety of spectroscopic methods, including UV−vis, $^1$H NMR spectroscopy, and mass spectrometry. Here, we have extensively used electrospray ionization mass spectrometry (ESI-MS), since we found it to be a remarkable method for a complete analysis of the situation in solution as previously proposed.[31]

From these data, it is clearly demonstrated that at least three oxo-bridged iron complexes are present in a $CH_3CN$:$H_2O$:acetate solution when ferric iron is chelated by 1 equiv of the EDTA analogue, **L1**: one tetranuclear complex (complex **1** in the case of **L1**) and two dinuclear oxo-bridged complexes. All of these complexes have their ferric ions coordinated by the two nitrogen and two of the four oxygen atoms of the ligand, and the oxygen atom of the oxo bridge and differ only by the sixth iron coordination site. One of the dinuclear complex has one molecule of water at each iron, the other one has an acetate bridging the two irons, and the tetranuclear complex is a condensation of two $\mu$-oxo diferric units linked by the bridging carboxylate moieties of the ligand. Obviously, the proportion of the complexes depended on the solvent. Only the stable tetranuclear complex was observed in pure acetonitrile. It was transformed into the bis aquo dinuclear complex in the presence of water and into the acetato-bridged dinuclear complex in the presence of small excesses of acetate.

Only the tetranuclear complex could crystallize, even from solutions where dinuclear complexes dominated. The three-dimensional structure could be determined by X-ray crystallography, in the case of the ligand **L1** (complex **1**). It revealed that, as described above, the carboxylate moieties of the ligand served to link two oxo-bridged diferric units. This is thus an original tetranuclear structure since it is the first example in which two dinuclear units are condensed exclusively through carboxylate bridges. In previously described examples the link was provided by a combination of oxo, hydroxo, and carboxylato bridges.[22] It should be noted that there are precedents in which acetato moieties of EDTA were found to link a $\mu$-oxo diiron complex to a metal ion.[32]

It was quite unexpected that incorporation of a methylene in the diamine chain (ligand **L3**) or in the glycinyl chain (ligand **L4**) resulted in molecules with no affinity for iron. During reaction with iron salts we did not find evidence for mono- or polynuclear complexes, demonstrating that the skeleton $O_2C-CH_2-N-CH_2-CH_2-N-CH_2-CO_2$ was absolutely required for iron chelation. There are certainly strict steric constraints which allow for very little variations of the tetradentate structure. For example, the carboxylate group can be changed to a pyridine, at least if the methylene is attached to the ortho position (ligand **L6**). On the other hand, more flexibility is possible at the benzyl branch, which lies away from the coordination sphere as suggested by the crystal structure of complex **1**, even though ligand **L7**, with methoxy groups in meta position, could not give rise to a pure diiron complex but rather a mixture of mono- and dinuclear complexes.

Our results also showed that these diiron complexes efficiently reacted with molecular oxygen in the presence of ascorbate. In this original reaction the ligand was almost quantitatively hydroxylated, with the incorporation of one oxygen atom derived from oxygen exclusively, at the ortho position of one phenyl ring. The resulting phenolate binds to the iron and stabilizes a mononuclear iron complex which is the final stable product of the reaction. Whereas a number of ligand oxidations have been observed with copper and manganese ligands,[33] there was no precedent for such a chemistry in the case of nonheme diiron complexes. Minor reactions occur at the methylene of the benzyl moiety, proving that the metal center has the potential for aliphatic C−H oxidation, at least in $\alpha$ position with regard to both a phenyl ring and a nitrogen atom. This should be further investigated.

Even though this hydroxylation reaction was also observed with hydrogen peroxide, we had evidence that $H_2O_2$ was not involved in the $O_2$-dependent reaction. In the case of ligand **L1**, which was extensively investigated in this study, we have clearly shown that no $H_2O_2$-dependent hydroxylation occurs within the tetranuclear complex **1**. The reaction takes place only in the presence of water or acetate, i.e., under conditions which desegregate complex **1** into diiron complexes, containing exchangeable $H_2O$ or acetato (complex **2**) ligands, respectively. This strongly suggested that only the diiron complex was catalytically competent for the hydroxylation reaction, because of its ability to bind $H_2O_2$. Binding of $H_2O_2$ is consistent with the observed saturation behavior of the reaction with respect to $H_2O_2$. The requirement of exchangeable sites within diiron complexes for peroxide activation has been previously demonstrated.[26] Oxidation of the ligand was favored by electron-donating substituents on the phenyl ring, as expected, confirming that the oxidizing intermediate species was electrophilic in nature (compare **L1**- and **L2**-based complexes).

Only in the case of the ligand **L6**, containing pyridine ligands in place of carboxylates, did the dinuclear complex not give rise to the mononuclear phenoxo−iron complex using both oxidizing systems. This points to the importance of carboxylates in the iron coordination sphere for oxidant activation, in agreement with the domination of aspartates and glutamates in the iron center of methane monooxygenase and ribonucleotide reductase.

No oxidation of ligands **L3** and **L4**, which were not able to generate a diiron complex, could be observed, further confirming the requirement of binding of **L*n*** to iron for an efficient hydroxylation.

In Scheme 1 is shown our proposal for the reaction mechanism. In the case of the $O_2$-dependent reaction, we have clearly demonstrated, in particular by ESI-MS, that reduction of the diiron complex results in the formation of mononuclear ferrous complexes. This is not surprising as the ligands used here are not binucleating and diferrous model complexes are prone to decompose into mononuclear species. The nature of the intermediate oxygen-bound active species is still speculative, as all attempts to detect such complexes by the ESI-MS technique developed by Kim et al.[19] were unsuccessful (data not shown), and further studies are required to identify it. EDTA analogues lacking oxidizable groups might be useful for accumulating an intermediate species and characterizing it. Such a strategy is reminiscent of the one used in the analysis of the active diiron complex of ribonucleotide reductase from *Escherichia coli*, named compound X, and involved in the oxidation of tyrosine 122 into a tyrosyl radical: mutation of tyrosine 122 to a less reactive phenylalanine residue resulted in the detection

(31) Andersen, U. N.; MacKenzie, C. J.; Bergesen, G. *Inorg. Chem.* **1995**, *34*, 1435.

(32) Gomez-Romero, P.; Jameson, B.; Borras-Almenar, A.; Escriva, E.; Coronado, E.; Beltran, D. *J. Chem. Soc., Dalton Trans.* **1988**, 2747 and references therein.

(33) (a) Kitajima, N.; Osawa, M.; Tanaka, M.; Moro-oka, Y. *J. Am. Chem. Soc.* **1991**, *113*, 8952. (b) Itoh, S.; Kondo, T.; Komatsu, M.; Oshiro, Y.; Li, C.; Kanehisa, N.; Kai, Y.; Fukuzumi, S. *J. Am. Chem. Soc.* **1995**, *117*, 4714. (c) Lee, D H.; Murthy, N. N.; Karlin, K. D. *Inorg. Chem.* **1996**, *35*, 804 and references therein.

**Scheme 1.** Proposed Mechanism for the Aromatic Hydroxylation of the Ligand **L*n*** Where the Bridge B in the Dinuclear Structure Is Unknown (one phenyl group has been omitted for clarity)

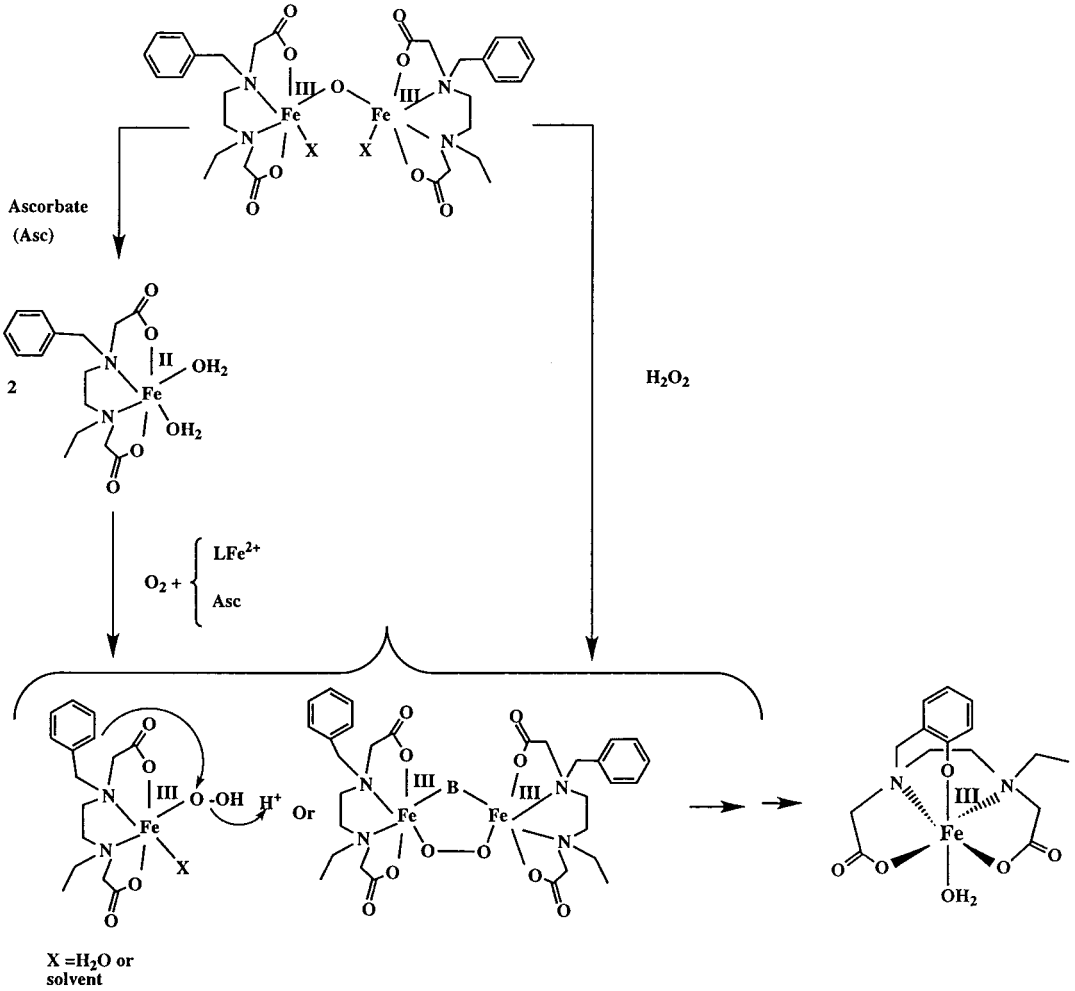


of larger amounts of compound X, suitable for spectroscopic characterization.[16]

Nevertheless, since the net result of the reaction is a two-electron oxidation and ascorbate, as an electron source, proved to be an important component of the system, the possible intermediates are the following: (i) a mononuclear ferric peroxo complex, derived from a one-electron reduction of the oxy complex; (ii) a dinuclear $\mu$-peroxo iron complex, derived from the coupling of the oxy complex with a mononuclear ferrous complex; (iii) a high-valent iron−oxo complex (not shown in Scheme 1), derived from (homolytic or heterolytic) cleavage of the peroxo complexes. The oxidation reaction works with $H_2O_2$ as well and probably goes through one of these complexes. In that case, a $\mu$-peroxo dinuclear structure is more likely to be on the pathway as there are several examples of well-characterized such complexes formed during reaction of diiron complexes with $H_2O_2$.[34]

All of these complexes are electrophilic and may be attacked directly by the nucleophilic electron-rich phenyl ring, in agreement with the full incorporation of $^{18}O$, in experiments carried out in the presence of $^{18}O_2$. If this mechanism is correct, it means that the active oxygen species is not (or slowly) exchangeable with water oxygen, as expected for peroxo complexes and sometimes observed in the case of iron−oxo complexes.[35] The fact that no incorporation of Br into the ligand from $CBr_4$ could be observed and no OH radicals could be trapped by the spin-trapping agent DMPO is more consistent with a concerted mechanism, with no intermediate free radicals. However, it is also possible that free radicals could be short-lived because they are so rapidly trapped by the adjacent phenyl ring of the ligand that no detection was possible. This entropic effect is qualitatively of the same nature as the efficient trapping of reactive intermediates by the substrate within active sites of enzymes.

Finally, whether or not the complex maintains its dimeric structure during reaction, it irreversibly loses it as soon as the phenol is formed and binds to iron. This is not surprising as phenolates are good electron-donating ligands which decrease the Lewis acidity of ferric iron and may prevent it from forming a dinuclear complex by binding an oxo bridge. This explains the mononuclear structure of the final product. It is also probably at the origin of its poor reactivity with $H_2O_2$ and explains why only one phenyl moiety was oxidized.

In conclusion, the dinuclear complex that can be prepared from EDTA analogues has many features in common with the iron center in methane monooxygenase and ribonucleotide reductase. First, it provides a coordination to the iron most comparable to that in the enzymes with a large proportion of carboxylate ligands. Second, it can efficiently activate molecular

(34) (a) Kim, K.; Lippard, S. J. *J. Am. Chem. Soc.* **1996**, *118*, 4914. (b) Dong, Y.; Yan, S.; Young, V. G., Jr.; Que, L., Jr. *Angew. Chem., Int. Ed. Engl.* **1996**, *35*, 618. (c) Ookubo, T.; Sugimoto, H.; Nagayama, T.; Masuda, H.; Sato, T.; Tanaka, K.; Maeda, Y.; Okawa, H.; Hayashi, Y.; Uehara, A.; Suzuki, M. *J. Am. Chem. Soc.* **1996**, *118*, 701.

(35) Lee, K. A. L.; Nam, W. *J. Am. Chem. Soc.* **1997**, *119*, 1916.

oxygen and carry out an aromatic hydroxylation. MMO oxidizes benzene into phenol[36] but there is no evidence for the formation of an iron−phenoxo complex, even though phenol has been shown to bind to the iron center of MMO.[37] Our reaction better mimics the $O_2$-dependent conversion of a tyrosine into dopa within a mutant of ribonucleotide reductase. In that case, the resulting catechol was found bound to the iron center.[16]

Finally, with these ligands, the substrate was brought at proximity to the metal center. As a consequence the hydroxylation was fast and almost quantitative. The reaction is thus much more efficient than the well-known related catalytic Udenfriend's system, consisting of ferrous ions, EDTA, ascorbic acid and dioxygen at neutral pH.[38] The complexes reported here might be useful tools for understand the hydroxylation mechanism of the reactions performed by these systems.

**Acknowledgment.** We thank Professor C. Béguin, Professor G. Serratrice for their expertise in p$K_a$ values determination and I. Beck and B. Le Guyader for their expertise in HPLC experiments.

**Supporting Information Available:** A listing of X-ray structure determination of 1 including tables of bond lengths and angles, atomic positional parameters, and final termal parameters (8 pages, print/PDF). See any current masthead page for ordering information and Web access instructions.

JA981123A

(36) Colby, J.; Stirling, D. I.; Dalton, H. *Biochem. J.* **1977**, *165*, 395.
(37) Andersson, K. K.; Elgren, T. E.; Que, L., Jr.; Lipscomb, J. D. *J. Am. Chem. Soc*. **1992**, *114*, 8711.
(38) Undenfriend, S.; Clark, C. T.; Axelrod, J.; Brodie, B. B. *J. Biol. Chem.* **1954**, *208*, 731.